Paleoceanography and Paleoclimatology

AGU ADVANCING EARTH AND SPACE SCIENCE

RESEARCH ARTICLE
10.1029/2021PA004289

A 1-Million-Year Record of Environmental Change in the Central Mediterranean Sea From Organic Molecular Proxies

Ariadna Martínez-Dios[1], Carles Pelejero[1,2], Sara Cobacho[1], Juancho Movilla[1,3], Jaume Dinarès-Turell[4], and Eva Calvo[1]

[1]Institut de Ciències del Mar, CSIC, Barcelona, Spain, [2]Institució Catalana de Recerca i Estudis Avançats, Barcelona, Spain, [3]Estació d'Investigació Jaume Ferrer, COB, IEO, Menorca, Spain, [4]Istituto Nazionale di Geofisica e Vulcanologia (INGV), Rome, Italy

Key Points:

- A molecular biomarker record covering the last 1 million years is presented, for the first time, in the Mediterranean Sea
- Sea surface temperatures in this new record from the Sicily Strait were consistently warmer than other records located further to the west
- Alternate peaks of alkenones and brassicasterol coeval to several sapropels suggest distinct proliferation of coccolitophores and diatoms

Supporting Information:

Supporting Information may be found in the online version of this article.

Correspondence to:

A. Martínez-Dios and C. Pelejero, amartinez@icm.csic.es; ariadnamartinezdios@gmail.com; carles.pelejero@icrea.cat

Citation:

Martínez-Dios, A., Pelejero, C., Cobacho, S., Movilla, J., Dinarès-Turell, J., & Calvo, E. (2021). A 1-million-year record of environmental change in the Central Mediterranean Sea from organic molecular proxies. *Paleoceanography and Paleoclimatology*, *36*, e2021PA004289. https://doi.org/10.1029/2021PA004289

Received 3 MAY 2021
Accepted 26 SEP 2021

Abstract The Mediterranean Sea is particularly sensitive to climate oscillations and represents a key location to study past climatic and oceanographic changes. One valuable source of paleoceanographic information is through molecular biomarkers in deep sea sediments. This approach has been applied in a number of studies in this basin, but only covering the most recent glacial/interglacial cycles. Here we present, for the first time in the Mediterranean Sea, a molecular biomarker record from the Strait of Sicily that covers the last million years until the present, almost continuously. We present data on alkenone derived $U^{K'}_{37}$ index sea surface temperatures (SST) and provide insights on the evolution of the phytoplankton community composition and terrestrial inputs through the analysis of the concentrations of alkenones, brassicasterol and long-chain alcohols. The $U^{K'}_{37}$-SST record followed a climatic evolution modulated by glacial/interglacial cycles with a marked increase in the 100 kyr-amplitude of the glacial cycles at ~430 ka, coincident with the Mid-Brunhes transition. In addition, SSTs were consistently higher compared with other records in the western Mediterranean, indicative of the progressive warming that surface waters experience along their transit from the Strait of Gibraltar to the Central Mediterranean. Regarding the concentrations of alkenones and brassicasterol, they displayed distinct alternate peaks, some of them coeval with the deposition of sapropels. This suggests that different environmental and oceanographic conditions characterized each sapropel which, together with changes in terrestrial inputs and the degree of oligotrophy, induced the alternate proliferation of coccolithophores and diatoms.

Plain Language Summary The Mediterranean Sea, located between subtropical and temperate latitudes, is a very sensitive area to changes in climate, becoming an ideal location for studying past climate changes. One valuable source of information about past ocean conditions are fossil molecules—or biomarkers—produced by microalgae or terrestrial plants, that end up buried in deep sea sediments. This technique has been widely used in the Mediterranean Sea to infer sea surface temperatures (SST), but only covering the last ~500,000 years. In this work, we studied a deep sea sediment core from the Strait of Sicily (Central Mediterranean), that covers a much longer time scale, the last million years until the present, almost continuously. By analyzing fossil molecules in this core, we were able to reconstruct SST and infer changes in microalgae community and their relationship with terrestrial inputs to the ocean. Our data indicate that the SST evolution in the Central Mediterranean followed global trends but with slightly warmer temperatures compared to other records in the Western Mediterranean. Moreover, the studied biomarkers pointed towards alternate periods of proliferation of diatoms and coccolitophores. Some of these events matched the Mediterranean sapropels which, particularly in the eastern basin, were times of significantly enhanced primary productivity, surface stratification and deep-water anoxia. We suggest that different environmental conditions during each sapropel, related to the nutrient supply and the degree of oligotrophy, may explain the alternate development of these algal groups.

1. Introduction

The Mediterranean Sea is a semi-enclosed sea located between the temperate and subtropical latitudes of the Northern Hemisphere and connected to the Atlantic Ocean through the Strait of Gibraltar (Figure 1).

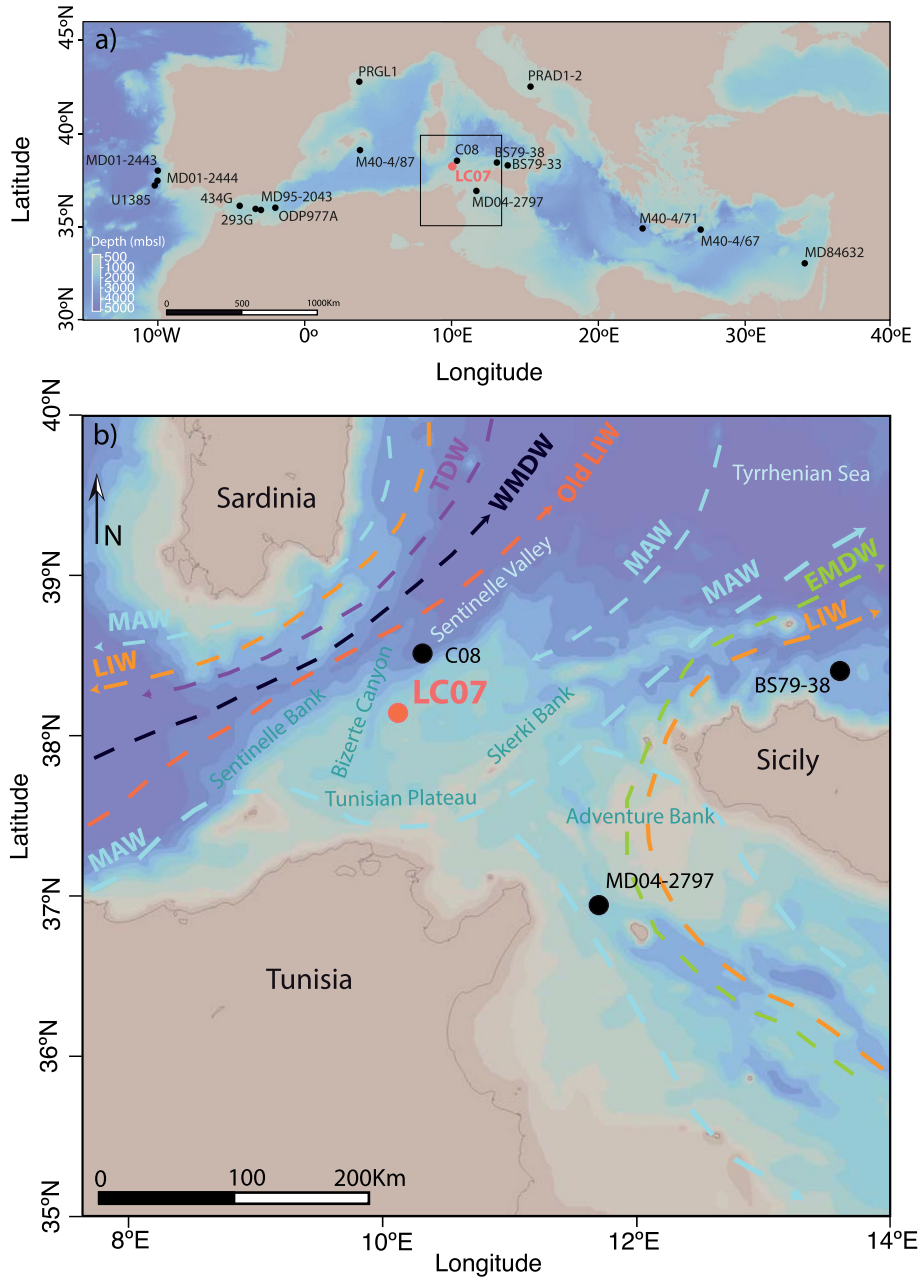

Figure 1. (a) Bathymetric map of the Mediterranean Sea with the location of the studied core (LC07) together with other cores for which, at least, the last glacial/interglacial cycle has been reconstructed using molecular biomarkers (see Table 1 for references). (b) Bathymetric map of the study area showing the location of core LC07 and a schematic representation of the most important ocean water masses and currents in the area (Astraldi et al., 2002; Jouini et al., 2016; Onken et al., 2003). Three additional sediment cores of relevance in the study area are also included (MD04-2797, Sicre et al., 2013; C08, Budillon et al., 2009; BS79-38, Cacho et al., 2001). Surface currents transport Modified Atlantic Water (MAW; light blue), while intermediate depths are occupied by Levantine Intermediate Water (LIW; orange). Greater depths are occupied by deep water from different origins: West Mediterranean Deep Water (WMDW; dark blue), Tyrrhenian Deep Water (TDW; purple) and Eastern Mediterranean Deep Water (EMDW; green) respectively. Bathymetry from GEBCO Compilation Group (2020).

Nowadays, it has an active thermohaline circulation driven by an overall excess of evaporation over precipitation and river runoff that creates a strong west-east gradient in surface temperature and salinity (Rohling et al., 2015). Its relatively small size, restricted communication with the open ocean and location between the monsoon system and the temperate westerlies confers to the Mediterranean Sea an extraordinary

Table 1
References of the Sediment Cores Shown in Figure 1a

Sediment core	Reference
PRAD1-2	Piva et al., 2008
MD95-2043	Cacho et al., 1999
BS79-38 and BS79-33	Cacho et al., 2001
293G and 434G	Rodrigo-Gámiz et al., 2014
PRGL1	Cortina et al., 2015, 2016
LC07	Dinarès-Turell et al., 2003
MD84-632	Essallami et al., 2007
M40-4/67, M40-4/87 and M40-4/71	Emeis et al., 2003
U1385	Rodrigues et al., 2017
ODP977A	Martrat et al., 2004
MD01-2443 and MD01-2444	Martrat et al., 2007
MD04-2797	Essallami et al., 2007 and Sicre et al., 2013

sensitivity to changes in global climate (e.g., Sprovieri et al., 2012). In this respect, the Mediterranean Sea is considered as one of the hot-spots for climate change in the world, where the future changes are expected to be most important (Giorgi, 2006). In this context, paleoceanographic data are very useful sources of information to assess climate sensitivity and potential impacts and consequences of present climate change.

Records of past climate changes in the Mediterranean have been documented through paleoceanographic reconstructions based on a variety of paleo-archives and proxies including marine biomarkers (fossil molecules) from deep sea sediments. Among molecular biomarkers, long-chain alkenones, synthesized by haptophyte algae, form the basis of a widely used paleothermometer, the $U^{K'}_{37}$ index (e.g., Herbert, 2003; Pelejero & Calvo, 2003). Alkenones, together with specific sterols, can also provide qualitative information on the speciation of phytoplankton, while long-chain alcohols and alkanes can be taken as indicators of terrestrial inputs to the ocean (e.g., Calvo et al., 2004, 2011).

Most of the Mediterranean Sea paleoceanographic reconstructions generated using molecular biomarkers only cover the last few glacial to interglacial cycles and the Holocene (Figure 1, Table 1). Nonetheless, they have already evidenced the particular sensitivity of the Mediterranean Sea to global climate changes during the late Quaternary. That is the case of the Western Mediterranean, which holds the two longest continuous records of $U^{K'}_{37}$-SST, the core ODP977A record, in the Alboran Sea, that extends back to ~250 ka (Martrat et al., 2004) and the record of core PRGL1, in the Gulf of Lions, which goes further back in time, reaching ~530 ka but with no Holocene (Cortina et al., 2015, 2016). These studies, together with those from Cacho et al. (1999) and Sierro et al. (2005), reported clear cold excursions during the last glacial period associated with the massive entrance of polar waters from the North Atlantic that led to brief, yet pronounced, negative $\delta^{18}O$ anomalies and large increases in the abundances of the polar foraminifera *Neogloboquadrina pachyderma* (sinistral).

The Eastern Mediterranean has also been studied from the perspective of molecular biomarkers in a number of cores (Figure 1, Table 1), but it lacks long, continuous, $U^{K'}_{37}$-SST reconstructions. In contrast, numerous efforts have been made in understanding the origin, timing and characteristics of the organic-rich layers known as sapropels, which periodically appear in the sedimentary sequences since mid-Miocene times (Taylforth et al., 2014). Although sapropels are more frequently and intensely developed in the eastern basin, sequences with similar characteristics have also been recorded in the central and western Mediterranean (Rohling et al., 2015 and references therein). These sequences are generally attributed to the recurrent pulses in African monsoon-related runoff (from the Nile River and North African systems) which cause stratification and bottom water anoxia, at times of precession minima (Grant et al., 2016). This freshwater forcing over the Mediterranean, controlled by precession, has shown to dramatically reduce the

Mediterranean Overturning Circulation (MOC; Bahr et al., 2015; Sierro et al., 2020), potentially altering density gradients that govern North Atlantic deep convection (Rogerson et al., 2012).

Here we present new records from the LC07 sediment core, retrieved from the Central Mediterranean, that covers the last million years until the Holocene. It records this period almost continuously, with the exception of a sediment gap between ~670 and ~590 ka (Dinarès-Turell et al., 2003). Given its location, at the connection between the two main Mediterranean sub-basins, and its time coverage, it is a valuable sedimentary sequence to investigate environmental changes across and after the two most important climate transitions of the Quaternary: the late Mid-Pleistocene Transition (MPT, base of the core until 700 ka) and the Mid-Brunhes Transition (MBT, ~430 ka), that caused a change in the periodicity and intensity of the climate cycles. In this sense, data from core LC07 could potentially provide new insights on how the Mediterranean Sea responded to orbitally-driven changes in global ice-volume and the African monsoon, and on how its response shaped global climate. We provide the first quasi-continuous $U^{K'}_{37}$ index sea surface temperature (SST) record covering the last 28 Marine Isotopic Stages (MIS) and draw inferences about the changes in terrestrial inputs and in phytoplankton community composition over this period. We discuss our data in the context of other alkenone-based SST records and highlight a series of correspondences with Mediterranean sapropels. Some questions we seek to answer in this study include: What was the variability of the $U^{K'}_{37}$ derived SSTs in the central Mediterranean over the last million years? How did the SSTs compare with other shorter records from the Mediterranean Sea? Were there any changes associated with the MPT and MBT? Was there an imprint in the molecular biomarker composition during sapropels in the Central Mediterranean? How can they inform us about possible phytoplankton changes during these events, and their environmental characteristics?

2. Study Area

2.1. Seafloor Topography

The Strait of Sicily, in the Central Mediterranean Sea, connects the eastern and western sub-basins of the Mediterranean Sea. The studied core, LC07 (more details in Section 3.1), was recovered from the western end of the Strait of Sicily, approximately equidistant (~100 km) from the Tunisian and Sardinian coasts, and at 200 km from Sicily (Figure 1). More specifically, the core was recovered from the Tunisian plateau, a wide extended area with a relatively gentle morphology and an average depth of less than 600 m (Mascle et al., 2004). The smooth surface of the plateau is interrupted by a number of irregular bathymetric features, such as the SSW-NNE oriented Sentinelle Valley in the northwestern end of the plateau. This valley is connected to the Bizerte Canyon, which limits the western end of the Tunisian Plateau (Aïssi, 2015). This canyon is not connected to the Tunisian margin, so it is not directly fed by any fluvial systems, but it drains the large Tunisian Plateau (Budillon et al., 2009). Another important feature in the area is the Skerki Bank, a 50 km long, SW-NE oriented ridge located approximately 80 km east of our core location. Due to its very shallow depth, reaching −0.5 m at Keith Ridge, the Skerki bank is known to alter the water flow paths (Onken et al., 2003; Sammari et al., 1999), and it has been the scene of numerous shipwrecks, becoming an important site from an archeological point of view (Ballard et al., 2000).

2.2. Currents and Water Masses

The NW sector of the Sicily Strait, as part of the connection between the two Mediterranean basins, is bathed by the confluence of distinct water masses (Figure 1) with intricate water mass exchanges, involving water mass transports of ~1.8 Sv and supporting speeds of up to 30 cm s^{-1} (Onken et al., 2003). For simplicity, the circulation in this region has been described as a two-layer exchange of surface Modified Atlantic Water (MAW; $T = 17°C$, $S = 37.2–38.2$, 0–200 m), brought by a jet of the Algerian-Tunisian Current, and Eastern Outflow Water, mainly composed of Levantine Intermediate Water (LIW; $T = 15°C$, $S = 38.7$, 200–500 m) and Eastern Mediterranean Deep Water (EMDW; $T = 13.6°C$, $S < 38.7$, ~800 m) (Astraldi et al., 2002; Bonanno et al., 2014). Surface processes at the location of LC07 are, therefore, strongly influenced by MAW, while the sediment core is bathed by LIW waters (Onken et al., 2003). Regarding the latter, the area receives, not only the recently formed LIW, but also a returning flow of old LIW and Western Mediterranean Deep Water (WMDW) formed in the Alghero-Provençal basin that spreads towards the Tyrrhenian Sea through

the Sardinia Channel, between the Sardinian slope and the Skerki Bank (Astraldi et al., 2002; Sammari et al., 1999). According to Onken et al. (2003), the shallow depths of the Skerki and Sentinelle banks seem not to affect MAW circulation, but they do apparently block and recirculate part of the western flowing LIW. Relevant to our study area is the wide, quasi-permanent cyclonic gyre located southeast of Sardinia that promotes vertical mixing and recirculation of the resident Tyrrhenian Deep Waters (TDW) (Figure 1) (Astraldi et al., 2002; Danovaro & Boero, 2019). Similar to the smaller cyclonic gyre located further north, to the East of Corsica, westerly winds are the driving force for these structures (de la Vara et al., 2019) and, during winter, both gyres are contained in a global cyclonic cell, sustained by wind-forcing, that extends over most of the basin (Iacono et al., 2021). In addition, the topographic features in the Sicily Strait are known to contribute, among other factors, to the formation of mesoscale structures that favor vertical mixing which ultimately yield nutrient cycling and seasonal productivity variations (Powley et al., 2017; Sammari et al., 1999).

2.3. Marine Production and Biology

In relation to nutrient chemistry and marine production, the Strait of Sicily separates the ultra-oligotrophic eastern basin from the oligotrophic western basin, with depth variable nutrient concentrations as a function of each water mass (Astraldi et al., 2002; Powley et al., 2017 and references therein). The Sardo-Tunisian plateau can be considered mesotrophic being dominated, in terms of phytoplankton, by nanophytoplankton (haptophytes and nanoflagellates) and picophytoplankton (cyanobacteria), with lower abundances of diatoms and dinoflagellates (Ciavatta et al., 2019). The vertical variability of phytoplankton in the area has been studied very scarcely so far, with one study based on pigments pointing towards highest phytoplankton biomass at around 70–100 m depth, coincident with the deep chlorophyll maximum (Brunet et al., 2007). As reviewed by Di Lorenzo et al. (2018), some studies observed relatively higher abundances of meso-zooplankton species in the Strait of Sicily than in surrounding areas. This is particularly evident in the western end, as a result of upwelling and water mixing associated with frontal systems and the advection of MAW, richer in nutrients, along the coast of North Africa (Rinaldi et al., 2014). In higher trophic levels, this situation promotes high species diversity and abundance in this region, which lays in the path of important migration routes for many species of turtles and cetaceans (Di Lorenzo et al., 2018).

3. Material and Methods

3.1. Sediment Core and Age Model

Marine sediment core LC07 (38°08.72′N, 10°04.73′E; 488 m water depth; 23.66 m length) was recovered in 1995 with a piston-corer device from the northwestern end of the Sicily Channel, in the Tunisian Plateau, onboard the R/V Marion Dufresne during the MAST II PALAEOFLUX Programme cruise (Figure 1). For this study, the core was sampled at the British Ocean Sediment Core Research Facility (BOSCORF) in Southampton, UK. The sediment core presents a foraminifer-rich sandy interval from 1,566 to 1,608 cm which was excluded from the analysis.

The age model is based on Dinarès-Turell et al. (2003), where $\delta^{18}O$ data of the planktonic foraminifer *Neogloboquadrina pachyderma* (dextral) were tuned to standard benthic $\delta^{18}O$ curves. Specific magnetic reversals (Matuyama/Brunhes, identified at 1,783 cm and upper Jaramillo at 2,245 cm) were also considered. In this study, the age model was slightly modified and updated by using the LR04 benthic stack (Lisiecki & Raymo, 2005) as the reference curve and the two magnetic reversals, encompassing a total of 48 pointers (Figure 2, Table S1 in Data Set S1). The age model provides average sedimentation rates of ∼2.6 cm/kyr for sections above the sandy interval and of ∼2.1 cm/kyr for samples below. The ∼5 cm sampling performed for molecular biomarkers yields resolutions of ∼1.9–∼2.4 kyr per sampled horizon, respectively.

3.2. Molecular Biomarker Analyses

Molecular biomarker (long-chain alkenones and alcohols, and sterols) were analyzed in a total of 415 sediment samples at Institut de Ciències del Mar in Barcelona, following published methods (Calvo et al., 2003; Kornilova & Rosell-Melé, 2003; Villanueva et al., 1997). Briefly, sediment samples were freeze-dried and

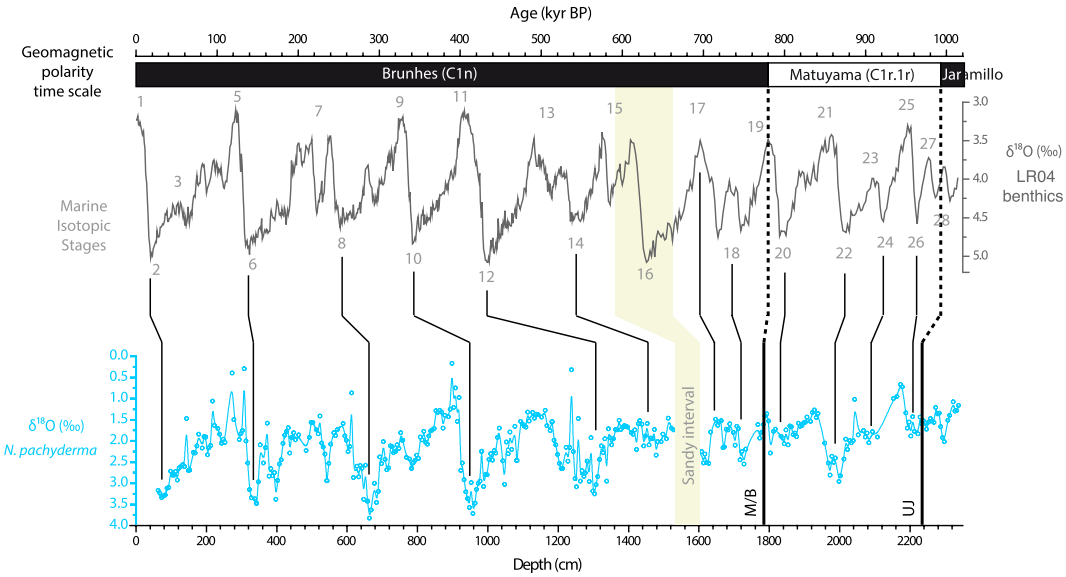

Figure 2. Age model of the studied core LC07 based on the tuning of *Neogloboquadrina pachyderma* (dextral) $\delta^{18}O$ (reversed axis, data from Dinarès-Turell et al., 2003) with the LR04 benthic $\delta^{18}O$ stack (reversed axis, Lisiecki & Raymo, 2005). The occurrence of a foraminifer-rich sandy interval and the position of the Matuyama/Brunhes (M/B) and upper Jaramillo (UJ) reversal boundaries (also used in the age model) are indicated. The solid line of the LC07 record is the cubic b-spline smooth of the original data (dots).

manually ground for homogeneity. About 6 g of freeze-dried sediment were loaded into 20 ml Teflon extraction vessels (MARSXpress, CEM Corp.) and *n*-nonadecan-1-ol, *n*-hexatriacontane and *n*-tetracontane were added as internal standards. Solid-liquid extraction of compounds was performed in a microwave digestion system (MARS 6, CEM Corp.) with dichloromethane. The evaporated extracts were left overnight with 6% potassium hydroxide in methanol at room temperature, in order to hydrolyze wax esters that may otherwise accumulate in the gas chromatography capillary columns. The neutral fraction was obtained after back extraction with *n*-hexane, three times, and it was left to evaporate under a gentle N_2 flow. Before full evaporation, the *n*-hexane extracts were washed with 1 ml of Milli-Q water to remove any KOH residue. After transferring the evaporated extracts to gas chromatography vials, they were derivatized with bis (trimethylsilyl) trifluoroacetamide. The extracts were then dissolved in toluene and injected in an Agilent 7890 Gas Chromatograph with a flame ionization detector (GC-FID) equipped with a VF-1 ms capillary column (60 m, 0.25 mm i.d., and 0.25 μm film thickness). The oven temperature programme was set at 90°C for 30 s and then raised at 20°C/min until reaching 160°C; it was then raised again at 6°C/min to 290°C, held for 40 min, raised again at 10°C/min to 310°C and held 6 min. The targeted compounds were quantified with reference to the internal standards.

3.3. Alkenone-SST Estimates

The $U^{K'}_{37}$ alkenone saturation index was calculated as $U^{K'}_{37} = C_{37:2}/(C_{37:2} + C_{37:3})$, where $C_{37:2}$ and $C_{37:3}$ are the di- and tri-unsaturated C_{37} alkenones, respectively. To convert the $U^{K'}_{37}$ ratios into temperature, we used the global surface water calibration of Conte et al. (2006) where $SST = -0.957 + 54.293\ (U^{K'}_{37}) - 52.894\ (U^{K'}_{37})^2 + 28.321(U^{K'}_{37})^3$. We chose this calibration because (a) it was also found appropriate in another SST reconstruction using alkenones for a sediment core in the Strait of Sicily, located ~200 km south west of core LC07 (Essallami et al., 2007; Sicre et al., 2013) but, more importantly, (b) because the SST provided by the core-top sample (18.3°C) matched the modern annual average SST (Figure 3, 18.7°C; World Ocean Atlas 2013, 0.25° grid data for 1955–2012, Locarnini et al., 2013). On the contrary, the widely used core-top calibration of Müller et al. (1998) provides a significantly colder core-top SST (16.3°C), similar to the global core-top calibration of Conte et al. (2006). This latter study also established a surface water calibration with samples from the Atlantic Ocean and the Mediterranean, which provides even a closer match to modern temperatures (18.6°C). However, given the standard error of these $U^{K'}_{37}$-SST calibrations (±1.2°C; Conte

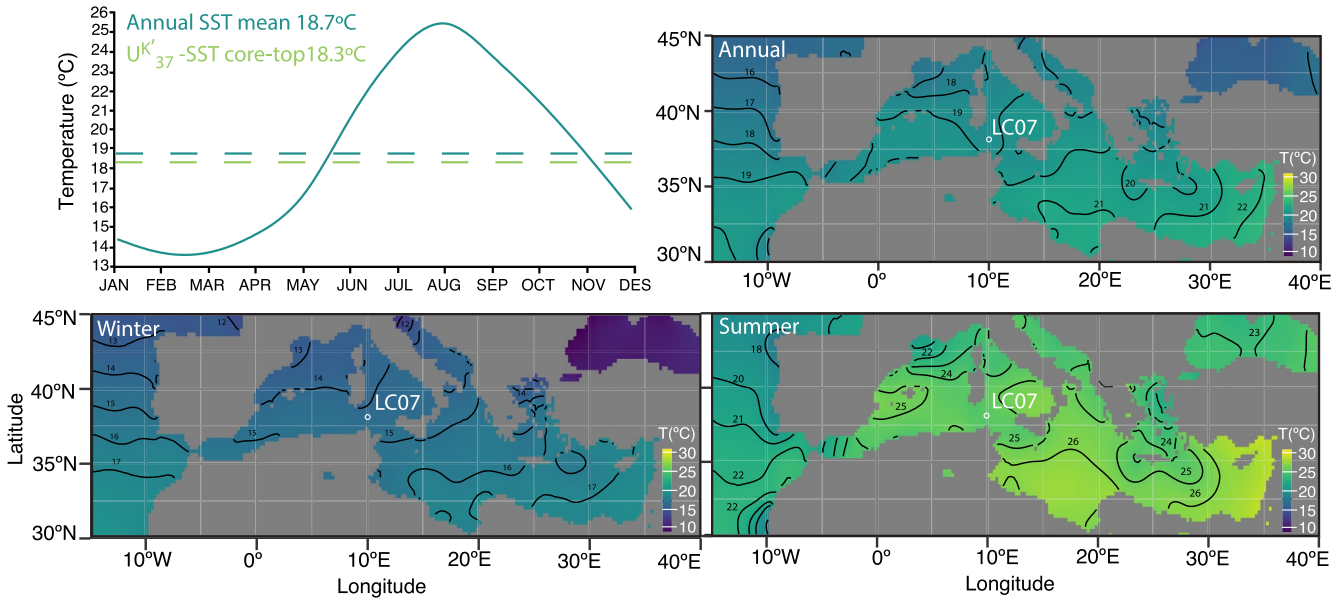

Figure 3. Sea surface temperatures annual cycle at the point closest to the LC07 location from the monthly 1-degree World Ocean Atlas 2013 data set and SST maps (annual, winter and summer means) using the 0.25-degree World Ocean Atlas 2013 data set (Locarnini et al., 2013). The white dots indicate the location of the LC07 core.

et al., 2006) and the minimal difference between the obtained SSTs, we opted to use the global surface water calibration, also used in the neighbor core (Essallami et al., 2007; Sicre et al., 2013). In the Mediterranean Sea, as it has been described in other areas (e.g., Atlantic Ocean, Müller & Fischer, 2001), $U^{K'}_{37}$-derived SST temperatures seem to reflect annually averaged surface temperatures, despite seasonal differences in phytoplankton productivity and the production of alkenones (e.g., Ternois et al., 1996). Regarding the analytical error, the standard deviation for replicate analyses of an in-house marine sediment standard was, at the most, ±0.3°C (σ).

3.4. Seawater Stable Oxygen Isotopic Composition

In order to obtain further insight on the hydrological cycle, $\delta^{18}O$ of seawater, ice-volume corrected ($\delta^{18}O_{sw\text{-}ivc}$), was calculated by subtracting the temperature and ice-volume effects from the $\delta^{18}O$ of *N. pachyderma,* using $U^{K'}_{37}$-SSTs and the ice sheet $\delta^{18}O$ component published by Bintanja et al. (2005), and the equation from Bemis et al. (1998):

$$\delta^{18}O_{sw-ivc} = \delta^{18}O_{N.\,pachyderma} - \delta^{18}O_{s.l} - \left(\left(SST - 16.5\right) / \left(-4.8\right)\right).$$

A + 0.27‰ offset correction was applied to $\delta^{18}O_{sw\text{-}ivc}$ in order to convert from V-PDB to VSMOW scale.

4. Results

4.1. $U^{K'}_{37}$-SST Record Over the Last Million Years

Over the last million years, $U^{K'}_{37}$-SST in the western end of the Sicily Strait oscillated following the global changes in ice volume, as seen by the agreement between the SST and the *N. pachyderma* $\delta^{18}O$ records (Dinarès-Turell et al., 2003; Figure 4) with the global benthic $\delta^{18}O$ stack (Lisiecki & Raymo, 2005). SST and *N. pachyderma* $\delta^{18}O$ show a remarkable similarity throughout the record with some exceptions, such as the most recent stages, particularly MIS 6 and 5, which display a smoother signal in the SST than in the $\delta^{18}O$ record. Between 160 and 140 ka, for example, an excursion towards light values in $\delta^{18}O$ was not paralleled by the SST record. In addition, some of the SST maxima in the interglacial stages after terminations were not always synchronous with the minima in planktonic foraminifera $\delta^{18}O$. On the other hand, after the MIS

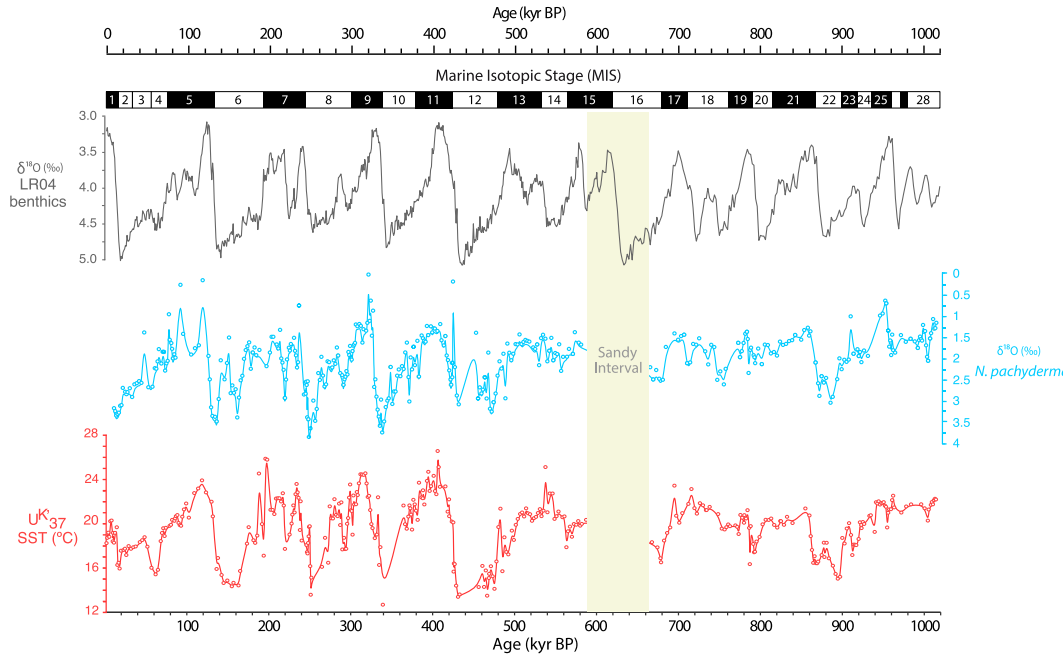

Figure 4. Dated records of *Neogloboquadrina pachyderma* (dextral) $\delta^{18}O$ (light blue, reversed axis, data from Dinarès-Turell et al., 2003) and $U^{K'}_{37}$-SST (red) for the studied core LC07 plotted together with the LR04 benthic $\delta^{18}O$ stack for comparison (light gray, reversed axis, Lisiecki & Raymo, 2005). The solid lines of the LC07 records are cubic b-spline smooths of the original data (dots).

10 to MIS 9 termination, maximum SST values were reached around 10 kyr later than the minimum in $\delta^{18}O$. For the rest of the core, especially during MIS 8 and 7 and the oldest sections below the sandy interval, both records varied very much in parallel.

Regarding temperature values, SST reconstructed in the northwestern Sicily Strait record oscillated between 12 and 26°C (Figure 4) with warmest interglacial temperatures between 18 and 26°C and coldest glacial temperatures ranging between 12 and 18°C (Table 2), depending on each MIS.

Looking at the whole record, SST and *N. pachyderma* $\delta^{18}O$ show a change in the behavior of the climate cycles at around 430 ka, coinciding with the Mid-Brunhes Transition (MBT). After 430 ka, the SST amplitude of the characteristic 100 kyr glacial/interglacial cycles tended to increase, similarly to what is reported globally in ice and marine sediment cores (Barth et al., 2018 and references therein). However, different to what is exhibited in ice cores and benthic $\delta^{18}O$ records, the increase in glacial/interglacial SST amplitude in our core after the MBT was more the result of a decrease in temperature minima during glacials than of an increase in the interglacial temperature maxima. In this regard, glacial stages before 430 ka tended to be warmer, exhibiting relatively temperate SST (average of 18°C) when compared to the minimum glacial SST values recorded after 430 ka (average of 14°C). We note, however, that the sandy interval of core LC07 includes MIS 16, a glacial stage that very likely had similar or lower SSTs than MIS 12, considering that the ice volume and extension during MIS 16 was similar to that during MIS 12 (Batchelor et al., 2019). The coldest SSTs for the whole record reached 12.6°C during MIS 10, followed by MIS 12 (13°C), MIS 6 (14°C) and the LGM (15.5°C). MIS 12 maintained cold temperatures over the longest duration of all glacial periods, exhibiting SST in the 13 to 15°C range (Figure 4). On the contrary, MIS 8 was punctuated by a relatively brief cooling at ~251 ka (13.2°C), while MIS 18 was the warmest glacial of the record, with an SST minimum of 19.4°C.

Regarding the interglacials of core LC07, they were characterized by a short period of maximum warmth followed by a progressive temperature decrease punctuated by rapid SST fluctuations. MIS 11, 9 and 7 were, on average, the warmest interglacials of the record (Table 2), while MIS 23 was the coldest interglacial, followed by the Holocene. MIS 13, despite showing relatively constant and fairly warm temperatures of ~20.2°C, recorded the minimum temperature of all interglacials, 15.5°C at 482 ka, although it is only a

Table 2
Average, Minimum and Maximum $U^{K'}_{37}$-SST (±Standard Error) for Each Marine Isotopic Stage in Core LC07

MIS	SST_{avg} (±SE)	SST_{min}	SST_{max}
1	19.0 ± 0.2	18.2	20.3
2	17.4 ± 0.3	15.7	19.6
3	17.8 ± 0.4	15.8	18.7
4	17.5 ± 0.9	15.2	19.5
5	20.9 ± 0.3	18.8	24.1
6	17 ± 0.7	14.0	24.7
7	21.7 ± 0.4	17.6	26.1
8	18.7 ± 0.4	13.2	22.3
9	21.7 ± 0.4	16.0	24.7
10	19.7 ± 0.9	12.7	21.7
11	22.7 ± 0.3	20.1	26.8
12	15.1 ± 0.4	13.0	19.6
13	20.2 ± 0.4	15.5	25.3
14	20.6 ± 0.4	17.7	22.8
15	19.9 ± 0.2	18.7	20.5
16	20.6 ± 0.7	16.3	22.8
17	20.8 ± 0.6	18.4	23.6
18	20.7 ± 0.3	19.4	21.9
19	19.8 ± 0.4	16.1	21.2
20	18.9 ± 0.4	17.2	20.4
21	19.1 ± 0.5	16.2	21.4
22	16.9 ± 0.4	14.8	19.5
23	18.7 ± 0.4	17.0	20.1
24	20.0 ± 0.2	19.2	20.8
25	21.5 ± 0.2	19.6	22.1
26	22.1 ± 0.3	21.5	22.6
27	21.3 ± 0.3	21.0	21.6

single data point. Other interglacials evolved over a more complex temporal evolution with multiple warm peaks separated by cold intervals, such as MIS 9 and 7. During the latter, in contrast to other interglacials, maximum warmth (26.1°C) was reached at the end of the interglacial (193 ka), prior to glacial inception. The warmest temperatures of the Holocene (20.3–20.2°C) were recorded at ~11–10 ka, but this interglacial is not fully covered by the planktonic foraminifera $\delta^{18}O$ data, so these ages should be taken with caution.

In relation to glacial/interglacial transitions (i.e., terminations), they were all characterized by the typical abrupt warming with large SST amplitude recorded also in the planktonic foraminifera $\delta^{18}O$ (Dinarès-Turell et al., 2003; Figure 4). As expected, after the MBT (~430 ka), terminations encompassed the largest amplitude SST changes (10–12°C), whereas before this the temperature difference over deglaciations was of only around 5°C, similar to Termination I, which was of exceptionally low SST amplitude. During Terminations V and II, the planktonic foraminifera $\delta^{18}O$ record displayed smaller amplitude changes than the record of SSTs (Figure 4). This is related, however, to the exceptionally light $\delta^{18}O$ values preceding both Terminations, which may be related to a freshening of seawater associated with a stronger influence of surface Atlantic Water (see below at the end of the Discussion).

4.2. Marine and Terrestrial Molecular Biomarkers and $\delta^{18}O_{sw\text{-}ivc}$

Figure 5 shows the temporal evolution in the concentration of several molecular biomarkers of marine and terrestrial origin, including C_{37} alkenones, 24-methylcholesta-5,22-dien-3β-ol (brassicasterol) and *n*-hexacosan-1-ol (C_{26}-ol), plotted together with planktonic foraminifera $\delta^{18}O$ and $U^{K'}_{37}$-SST. C_{37} alkenones and brassicasterol are produced by microalgae and are often interpreted as proxies of haptophyte and diatom export production, respectively. The synthesis of long-chain alkenones in the open sea is restricted to a few haptophyte species (Herbert, 2003 and references therein). In relation to brassicasterol, it is abundant in particular in pennate diatoms (Rampen et al., 2010), but other microalgae including haptophytes can also synthesize it (Volkman et al., 1998). In this study, we focus our interpretations on time periods when both microalgae proxies were decoupled, thus suggesting a different algal origin, haptophytes for alkenones and diatoms for brassicasterol (e.g., Calvo et al., 2004, 2011). Finally, even carbon number long-chain *n*-alcohols are found in leaves waxes of higher plants and ultimately reach the open sea transported by wind or through continental runoff (Eglinton & Eglinton, 2008). In this study, for simplicity, only the C_{26}-ol homolog was presented and interpreted as a proxy of terrestrial inputs.

Regarding the marine compounds, downcore concentrations in C_{37} alkenones and brassicasterol present a number of differences (Figure 5). Looking at the whole record, alkenones displayed higher concentrations for the sections older than 430 ka, while brassicasterol showed generally higher values after 430 ka. Before this time, brassicasterol displayed rather low levels, with average concentrations of 70 ng/g with small fluctuations. In addition, and particularly during the most recent half of the core, alkenones and brassicasterol evolved independently of each other, often displaying asynchronous peaks. The alkenone sharp peak at 330–315 ka, for example, occurred during a period of minimum concentrations in brassicasterol, while the brassicasterol broad maximum at 210–190 ka had no parallel in the alkenone record. These asynchronous modes of variability suggest a different evolution of the phytoplanktonic community over time in the studied location.

When comparing the marine biomarkers with the record of the terrestrial *n*-alcohol, it is worth to remark the close parallelism of the C_{26}-ol record with brasssicasterol concentrations but not with the alkenones

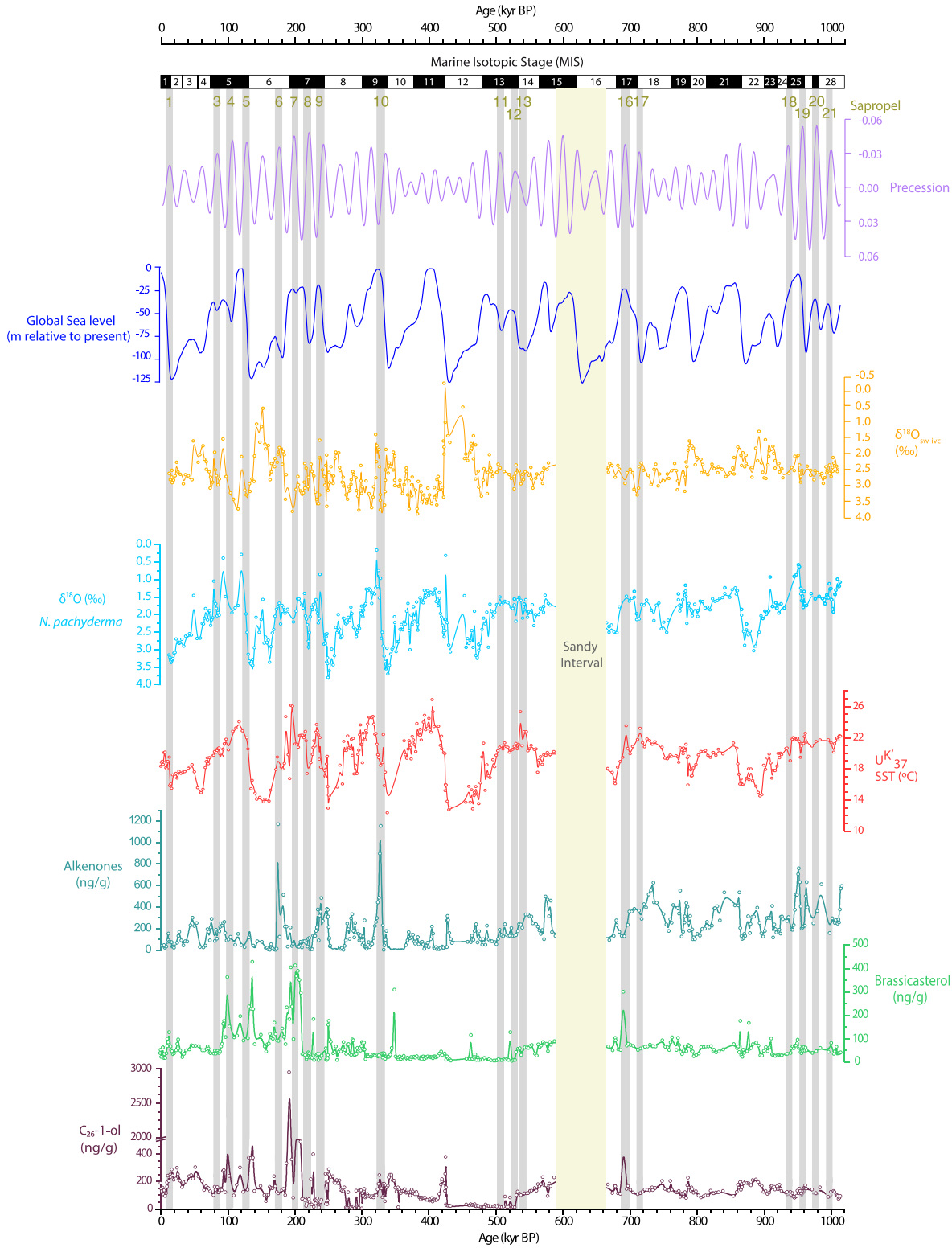

Figure 5. Composite of records from the studied core LC07. From top to bottom: Precession (purple, reversed axis, obtained from Laskar, 1990), global sea level (dark blue, Bintanja et al., 2005), $\delta^{18}O_{sw\text{-}ivc}$ (orange, reversed axis, see text for calculations), *N. pachyderma* (dextral) $\delta^{18}O$ (light blue, reversed axis, Dinarès-Turell et al., 2003), $U^{K'}_{37}$-SST (red), and concentrations of long-chain alkenones (sea green), brassicasterol (lime green) and hexacosan-1-ol (purple). Gray vertical bars indicate Mediterranean Sea sapropels based on the dates from Ziegler et al. (2010) and Konijnendijk et al. (2014). Note that the solid lines of the LC07 records are cubic b-spline smooths of the original data (dots).

(Figure 5). Some of the peaks in concentrations of C_{26}-ol and brassicasterol are synchronous, such as those at 99 ka, 136 ka, 192 ka and 205–209 ka, suggesting a possible link between terrestrial inputs and diatom development. Interestingly, many of the peaks in the proxies coincided with the timing of the Mediterranean sapropels, suggesting specific marine conditions in the Central Mediterranean during these events that may have favored in different ways the proliferation of haptophytes and diatoms (Figure 5). For example, the two more prominent peaks in the alkenones concentration record at 327 ka and 173 ka occurred contemporary with the deposition of sapropels S10 and S6, respectively. On the other hand, brassicasterol peaks at 690 ka and 99 ka occurred during the deposition of S16 and S4, respectively. For the most recent 50 kyr, alkenones and brassicasterol concentrations showed similar patterns, with two excursions at 26 ka and 12 ka, the latter contemporary to S1 deposition.

To illustrate the role of precession in modulating the development of sapropels (e.g., Grant et al., 2016), in Figure 5 we have plotted the evolution of this orbital parameter for comparison. As it can be seen, most of the sapropels coincide with minima in precession (and thus maxima in boreal summer insolation). The widely suggested explanation for this connection is that this orbital configuration led to northward shifts in the ITCZ, so the summer monsoon rain belt over North Africa migrated to the north. The associated enhanced precipitation led to freshwater inputs particularly in the eastern Mediterranean and to stratification of the water column, culminating with the development of sapropels. In order to investigate whether changes in salinity may have also characterized the Central Mediterranean during sapropels, we calculated the $\delta^{18}O_{sw\text{-}ivc}$ from the subtraction of the SST and ice volume components of the planktonic foraminifera $\delta^{18}O$ in core LC07 (Figure 5). Even though for some of the sapropels there seems to be small decreases in salinity (e.g., S17, S10, S9, S8, S6), the most prominent excursions towards sea-surface freshening occurred during periods when no sapropels developed (e.g., MIS 12 and late MIS 6). Hence, according to this, the widely reported seawater freshening exhibited in the Eastern Mediterranean during sapropels did not characterize so directly the Central Mediterranean.

5. Discussion

5.1. Long-Term SST Evolution in the Mediterranean Region

Over the last million years, SST in the Central Mediterranean has been modulated, to a large extent, by the evolution of glacial/interglacial cycles, as seen by the close correspondence between LC07 core SST and both local and global $\delta^{18}O$ data (Figure 4). For the most recent past, this parallelism has already been reported in other basins of the Mediterranean Sea (e.g., Cacho et al., 1999). In Figure 6, LC07 $U^{K'}_{37}$-SST are

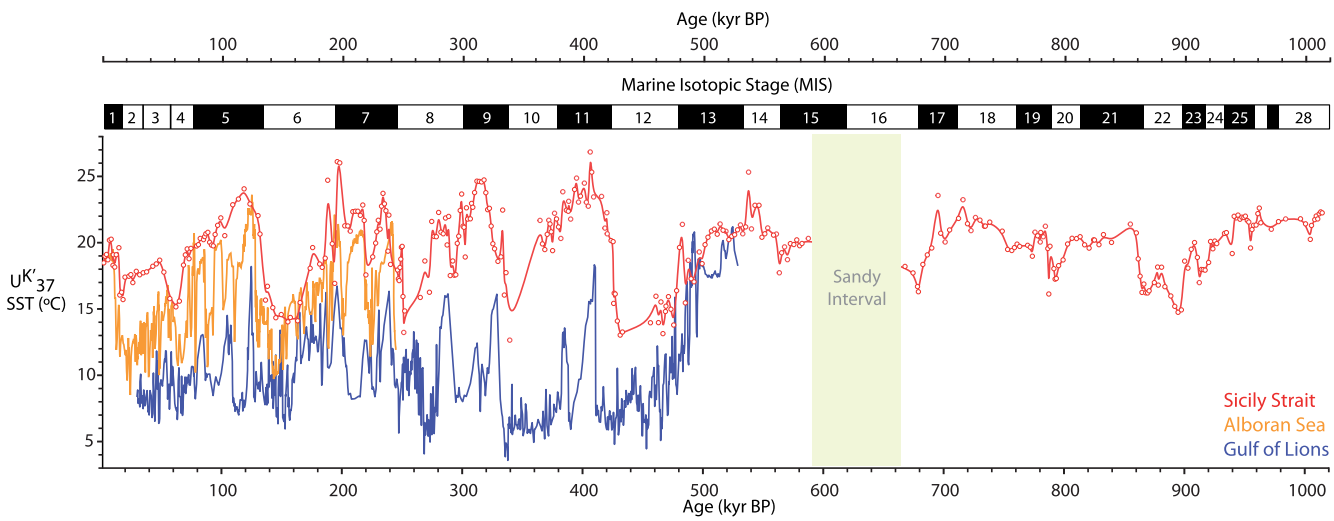

Figure 6. Comparison of the $U^{K'}_{37}$-SST record from the studied core LC07 (red) with the $U^{K'}_{37}$-SST from the Gulf of Lions (blue, PRGL1, Cortina et al., 2015, 2016) and the Alboran Sea (orange, ODP977A, Martrat et al., 2007). Note that $U^{K'}_{37}$-SSTs from the Alboran Sea and the Gulf of Lions were obtained with Müller et al. (1998) global calibration whereas the $U^{K'}_{37}$-SSTs from core LC07 were obtained with the global surface calibration of Conte et al. (2006) (see main text). The solid line of the LC07 record is the cubic b-spline smooth of the original data (dots).

compared with the two longest alkenone-based SST reconstructions published so far in the Mediterranean Sea (Martrat et al., 2004 in the Alboran Sea; Cortina et al., 2015, 2016 in the Gulf of Lions). As it can be seen, paleo SST in the Central Mediterranean show remarkably similar glacial/interglacial fluctuations to those in the Alboran Sea, highlighting a basin-wide temperature response to global ice-volume changes and climate. In relation to the Gulf of Lions, although the pace of the major changes is similar, SST in the Central Mediterranean was consistently higher and the recorded changes less abrupt.

Interestingly, $U^{K'}_{37}$-SST in the Strait of Sicily displayed consistently higher absolute values than the other records (Figure 6), indicative of the progressive warming that surface waters experienced during their transit from the Strait of Gibraltar and the Alboran Sea (Martrat et al., 2004), through the African Margin towards the Central Mediterranean. Recent studies on the abundance of specific calcareous nanoplankton have documented the persistence of this west-east temperature gradient during the middle and late Pleistocene (Marino et al., 2018 and references therein), due to the different insolation affecting the Mediterranean sub-basins (Sprovieri et al., 2012).

The LC07 (Sicily Strait) and ODP977A (Alboran Sea) locations experienced particularly similar SST values at specific periods, such as the 170 to 150 ka interval, and deglaciations evolved in apparent synchrony in both sites. During the Holocene, SST recorded in the Alboran Sea (e.g., MD95-2043 core, Cacho et al., 2002; and ODP977A core, Martrat et al., 2007) also reached similar magnitudes (18–19°C) to those at LC07 and further south-east in the Sicily Strait (MD04-2797 core, Sicre et al., 2013), pointing towards a significant homogeneity of surface waters at these locations during this period and, in general, during interglacials. This situation would have also characterized the Tyrrhenian Sea, at least the southeastern side, as suggested by two $U^{K'}_{37}$-SST reconstructions in this region (BS79-33 and BS79-38, Cacho et al., 2002, Figure 1). Differently, during glacial times, SST gradients between the Sicily Strait and the Alboran Sea intensified. This was particularly evident during the LGM, when the Alboran Sea and the Sicily Strait displayed a very different temperature range, indicative of a different sensitivity of the glacial cooling in both Mediterranean regions at this time. The North Atlantic cooling during glacials impacted more importantly the Alboran Sea as compared to other Mediterranean regions further East (Cacho et al., 2001, 2002; Martrat et al., 2007).

The $U^{K'}_{37}$-SST records of the Sicily Strait (LC07) and the Gulf of Lions (PRGL1) present more noticeable differences (Figure 6). On average, SST was much colder in the Gulf of Lions. Nowadays, this region experiences intense cooling in winter, that recurrently promotes the formation of dense waters that cascade to depth (e.g., Puig, 2017 and references therein). Similarly, during glacial times, the intensified north-westerly winds (Tramontane and Mistral) over the Gulf of Lions, linked to the southward migration of the polar front, led to the extremely cold SSTs observed in the PRGL1 core record (in some cases apparently reaching SST below 5°C, Figure 6, Cortina et al., 2015, 2016). These extreme glacial coolings, however, did not extend towards the Central Mediterranean, where the recorded SST was much milder (Figure 6). Interestingly, during MIS 13 and the start of the transition to MIS 12 at around 500 ka, SST recorded at both sites was very similar, so perhaps this pronounced Central to Northwest Mediterranean thermal differentiation started at around that time. Indeed, the finding that MIS 13 SST was the warmest period in the entire PRGL1 record (reaching ~20°C; Cortina et al., 2016) was interpreted by the authors as the result of a more northward position of the Inter-Tropical Convergence Zone (ITCZ) in winter at this time, which would have blocked the penetration of the cold north-westerlies winds. However, recent results from pollen analysis in the southwest Iberian Margin (site U1385, Figure 1) inferred that the westerlies strongly affected the western Mediterranean region during MIS 13 (Oliveira et al., 2020). In fact, in core LC07, similar to SSTs derived from foraminiferal assemblages from the Alghero-Balearic Basin (ODP 975, Girone et al., 2013) and also to $U^{K'}_{37}$-SSTs from site U1385 (Figure 6, Rodrigues et al., 2017), MIS 13 was not the warmest interglacial, exhibiting SSTs colder than MIS 11 and MIS 5.

Overall, due to its location at the confluence of different water masses connecting the western and eastern Mediterranean basins, with an important influence of the surface water recirculated in the Tyrrhenian Sea, but also considering the low resolution of the record, LC07 exhibits a particularly smoothed climatic signal as compared to other regions at the boundaries of the Mediterranean Sea. Indeed, the southern end of the Strait of Sicily itself seems to have been more sensitive to glacial cooling, reaching 8.5°C during the LGM (MD04-2797, Sicre et al., 2013). This location lays under the direct influence of the cold MAW during glacial times, whereas LC07, further northwest, may have been more affected by the recirculation of surface

warmer waters in the Tyrrhenian Sea, transported from the Eastern Mediterranean. In the southern end of the Sicily Strait, upwelling may have also had an influence in cooling surface waters, a year-round feature well described in modern times (Béranger et al., 2004).

For ages older than ~500 kyr, so far there are no other published continuous $U^{K'}_{37}$-SST records in the Mediterranean Sea to be able to draw comparisons with the LC07 record. During the 1–0.5 Ma period, the $U^{K'}_{37}$-SST record for core LC07 displays a glacial/interglacial climatic variability with smaller SST fluctuations (16–23°C), a feature that is even more evident during the period between MIS 28 to MIS 24 (20–23°C, Figure 6). This older half of the core includes the MPT, which involved a progressive shift from a 41 to 100 kyr periodicity dominating the ice volume record, accompanied by an intensification of glacial stages (Pena & Goldstein, 2014 and references therein). The LC07 $U^{K'}_{37}$-SST highlight MIS 22 as the first pronounced and maintained glacial cooling of the record, which was coeval with the first major Pleistocene glaciation in the Alps, as documented, for example, in a long record from the Po Plain (Muttoni et al., 2007). This involved drastic fluvial reorganizations that led to the development of large-scale submarine canyons in the Mediterranean basin (Mauffrey et al., 2017), as well as to major vegetation changes that included the demise of Tertiary forest species (Tzedakis et al., 2006). During MIS 21–17, increased aridity and hence higher salinity in the Eastern Mediterranean has been linked to enhanced Mediterranean Outflow Water (MOW) (Bahr et al., 2018). These dry conditions must have been especially intense at around 900 ka, matching a period of strong MOW production (Bahr et al., 2018).

By 700 ka, at the end of the MPT, SSTs at LC07 oscillated between 22 and 24°C, the warmest of the previous 300 kyr (Figure 6), preceding the intensification of the glacial/interglacial cycles and witnessing an exceptional expansion of forests in Southern Europe (Sánchez-Goñi et al., 2019). Starting in MIS 17, a reactivation of the North Atlantic circulation took place triggering the advection of relatively warm water to high latitudes providing humidity for the growth of the Northern Hemisphere ice-sheets that culminated with a maximum extension during MIS 16 (Martín-García et al., 2018). Unfortunately, the presence of a foraminifer-rich sandy interval encompassing MIS 16 prevents us from inferring climatic conditions at the LC07 location during this period. Similar winnowed deposits and hiatuses have been reported in the Gulf of Cádiz during previous periods at around 900 ka, being related to MOW intensification (Bahr et al., 2018 and references therein). A closer inspection to seismic profiles in the area revealed smooth, continuous strata surrounding the LC07 location, that is, an absence of abrupt geological features (Camafort et al., 2020). We therefore interpret this interval as a winnowed lag deposit as in Dinarès-Turell et al. (2003) and Camafort et al. (2020), an event probably caused by the removal of the fine sediment fraction due to strong bottom currents and an invigorated MOC. Extreme aridity (and hence stronger MOC) was indeed reported during glacial MIS 16 at Tenaghi Philippon (NE Greece) through the increased abundance of grassland pollen (Tzedakis et al., 2006).

Overall, the new $U^{K'}_{37}$-SST here presented, extending back to more than 1 Ma, gains further significance in the context of the current absence of SST records for the Mediterranean Sea extending back to this age. The LC07 SST record in the Central Mediterranean should help contextualize other terrestrial/marine reconstructions in the Mediterranean region in this time frame and, overall, highlights the role of marine currents and circulation in connecting this basin to the Atlantic Ocean, and in homogenizing or differentiating the thermal properties among all basins and sub-basins of the Mediterranean Sea.

5.2. SST Evolution in a Broader Context

The closest $U^{K'}_{37}$-SST record spanning the same time period covered by core LC07 is one from the South West Iberian Margin, a composite of the cores MD01-2443/4 and U1385 (Martrat et al., 2007; Rodrigues et al., 2017). In this section we broaden the context of the LC07 record by drawing comparisons between these two records (Figure 7).

In the Iberian Margin, SST was consistently colder than in the Central Mediterranean, with differences of up to 10ºC during specific glacial cold excursions in the Atlantic (Figure 7). In addition, the Iberian Margin record exhibited much higher temporal variability than the Central Mediterranean. This may be in part due to the higher sedimentation rates and resolution of this core as compared to the LC07, but this area is also known to be strongly influenced by subpolar waters recurrently brought by the Portugal Current as a result

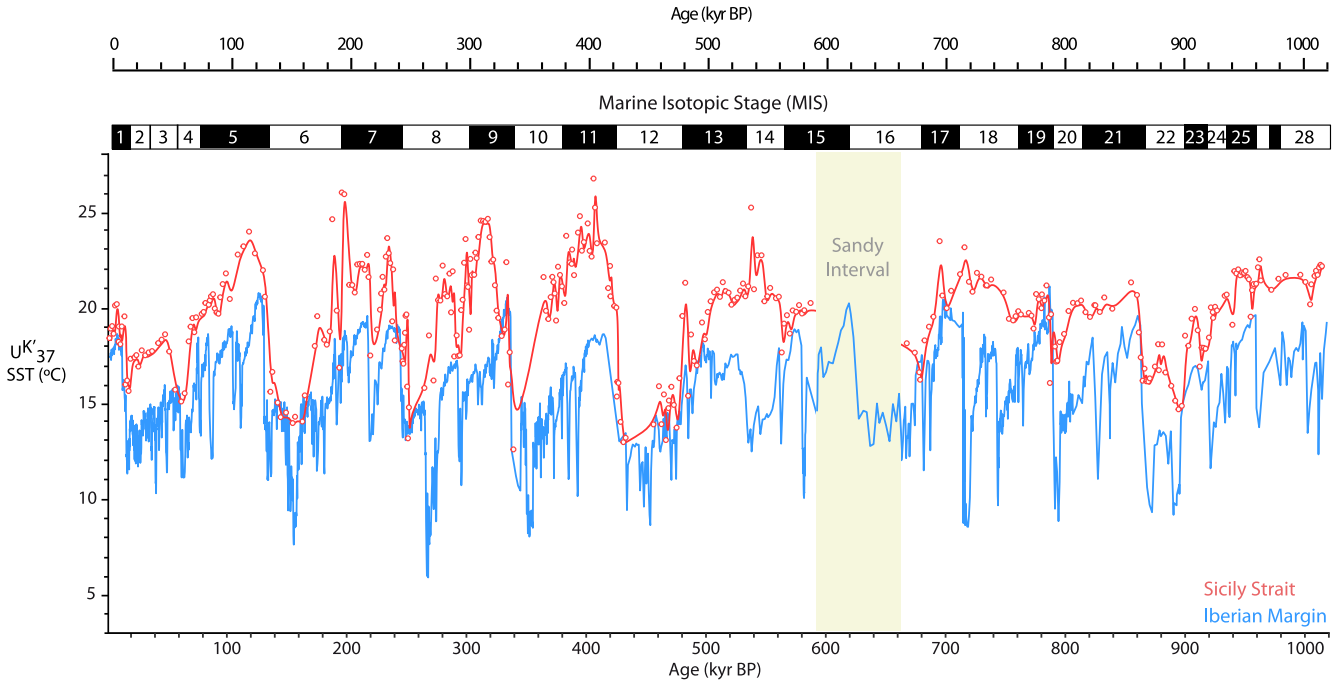

Figure 7. Comparison of the $U^{K'}_{37}$-SST record from the studied core LC07 (red) with the $U^{K'}_{37}$-SST record from the Iberian Margin (blue, composite of cores MD01-2443/4 and U1385, Martrat et al., 2007; Rodrigues et al., 2017). Note that $U^{K'}_{37}$-SSTs in the Iberian Margin were obtained using the Müller et al. (1998) calibration whereas the $U^{K'}_{37}$-SSTs from core LC07 were obtained with the global surface calibration of Conte et al. (2006) (see main text). The solid line in the LC07 record refers to the cubic b-spline smooth of the original data (dots).

of the southward migration of the Polar Front. The South West Iberian margin is thus very sensitive to the North Atlantic cooling, especially during glacial stages and terminations (Rodrigues et al., 2017).

During glacial periods, the sea-level low stand and sluggish Atlantic Meridional Overturning Circulation could have lowered the volume and velocity of MAW crossing the Strait of Gibraltar and reaching the Central Mediterranean, effectively decoupling the Iberian Margin from the Sicily Strait. As a result, differences in the timing of the coldest episodes are observed between the two records (Figure 7). Also, while the southward deflection of the polar front and the arrival of subpolar waters during late MIS 8 and MIS 6 (Rodrigues et al., 2017) led to rather extreme SST minima in the Iberian Margin of 6°C and 8°C, respectively, SST recorded in LC07 stayed above 14°C for both periods (Figure 7). In contrast, in the Strait of Sicily, the lowest glacial temperatures were observed during MIS 12, a glacial period which is considered to have been exceptionally cold, with a global ice volume ~15% greater than during the LGM (Batchelor et al., 2019; Vázquez-Riveiros et al., 2013). The MIS 12 has been reported to have been especially harsh in the Mediterranean region (Regattieri et al., 2016 and references therein), and was also the coldest glacial in the foraminiferal SST record from core ODP 975 in the Western Mediterranean (Girone et al., 2013).

Interestingly, similar SSTs were exhibited in the Iberian Margin and Central Mediterranean during certain periods, especially during late glacial stages and terminations (e.g., MIS 22 to 21, MIS 20 to 19, MIS 12 to 11, MIS 10 to 9, MIS 8 to 7, MIS 6 to 5, and the Last Deglaciation, including the Holocene, Figure 7). This may be the result of a stronger inflow of Atlantic surface waters into the Mediterranean Sea, linked to the sea level rise associated with deglaciations and an enhanced MOC.

Regarding the interglacials, large differences are observed between the Iberian Margin and the Central Mediterranean. The interglacials of the last 1 Ma are generally characterized by warm temperatures (Figure 7), high sea level and vigorous overturning circulation (Berger et al., 2016). Therefore, a strong oceanographic coupling between the Iberian Margin and the Central Mediterranean would be expected. However, SST at both sites differs in the absolute values and in the timing of the warmest maxima, suggesting that local influences may come into play. In this sense, warmer SST in the Central Mediterranean is in accordance with the strong W-E temperature gradient that occurs in the whole basin as a result of the latitudinal differences

in insolation between the two sub-basins (Sprovieri et al., 2012). For instance, MIS 11, known to have been among the longest and most intense interglacials of the Pleistocene (Berger et al., 2016), but suggested to have been moderately warm in the western Mediterranean (Oliveira et al., 2016), had still a profound impact in the SSTs in the Central Mediterranean, rising them up to 26°C (Figure 7). In addition, the SST maximum of MIS 7 is coeval with the deposition of sapropel S7, suggesting that water column stratification may have played an important role in enhancing surface warming at this time. In contrast, MIS 9 and MIS 5 appear to have been the warmest interglacials in the Iberian Margin (Figure 7). Enhanced warming in this region during specific interglacials may be attributed to a stronger influence of the Azores Current, as suggested by other records from the Southern Iberian Margin in the case of MIS 5 (Salgueiro et al., 2010). This idea is supported by a $U^{K'}_{37}$-SST record from a core near the Azores Islands (Calvo et al., 2001), the source region of the Portugal Countercurrent, which exhibited especially high SSTs during MIS 7 and 5.

Overall, the $U^{K'}_{37}$-SST record of the Strait of Sicily, as compared with the Iberian Margin, generally contains a global climatic signature of the last 1 Myr but with specific regional singularities in certain glacial and interglacial stages.

5.3. Marine and Terrestrial Biomarkers and Links to Sapropels

The concentrations of our selected molecular biomarkers of terrestrial and marine origin in core LC07 oscillated over the last million years following different patterns and evolutions (Figure 5). As opposed to the $U^{K'}_{37}$-SST record, a clear glacial/interglacial cyclicity was not evident in the biomarker records. Instead, they evolved more in the form of distinct peaks emerging from rather constant baselines (Figure 5). Interestingly, several of these peaks were contemporary with the deposition of sapropels in the Eastern Mediterranean Sea (Figure 5).

Sapropels have generally been attributed to drastic increases in precipitation and runoff from rivers to the Mediterranean Sea, related to the northward displacement of the monsoon rain belt over North Africa (Amies et al., 2019 and references therein). One of the main fresh water contributors to the Mediterranean Sea during sapropels was the Nile River which, for example during sapropel S5, discharged up to 9 times more water than during modern times, before the Aswan damming (Amies et al., 2019). In addition to the Nile River, a number of North African paleo-rivers have also been suggested to have played a role (Duhamel et al., 2020; Osborne et al., 2010; Wu et al., 2016, 2018) and even other rivers debouching into the Mediterranean Sea from the northern coastlines (Pasquier et al., 2019; Toucanne et al., 2015). Increased seasonal precipitation at times of sapropel formation has also been confirmed from the reconstruction of changes in vegetation through palynological studies (Rossignol-Strick & Paterne, 1999; Zwiep et al., 2018).

In core LC07, the concentration of the terrigenous proxy C_{26}-ol was generally low until 700 ka. After this age, several recurrent peaks of C_{26}-ol, at times of $\delta^{18}O$ minima, were likely related to enhanced monsoon-related river runoff to the Mediterranean Sea that occurred during sapropels. This could have been the case during sapropels S16, S5, S4 and possibly S7 (Figure 5), pointing thus towards a predominantly fluvial component of the terrigenous inputs to the core location at these times. After ca 350–400 ka, the concentration of C_{26}-ol was generally higher. This matches with the inferences reported for the Central Mediterranean Sea based on clay mineralogy, which indicated a change from a mainly eolian (Saharan dust) to a fundamentally fluvial source of the terrigenous material to this area at around 700 ka, and a large increase in terrigenous flux after 350 ka (Zhao et al., 2016). As suggested in this study, this last change may have been induced, in part, by the rapid tectonic uplift in the Calabrian Arch, promoting an important drainage in the Apennine fluvial system. Interestingly, the maxima in brassicasterol and C_{26}-ol concentrations during S16 at around 700 ka match the strong development of the Mediterranean forest in SW Iberia recorded from pollen at site U1385, indicative of humid conditions (Sánchez-Goñi et al., 2019).

Such riverine nutrient upload may have fueled the recurrent increases in marine primary productivity that have often been associated with sapropels (Rohling et al., 2015 and references therein). In core LC07, several maxima in the concentration of marine biomarkers occurred at times of sapropel events, lending support to the idea of increased marine production during these events (Figure 5). Interestingly, major alkenones and brassicasterol peaks were not synchronous, matching different sapropels (Figure 5). For example, the two most prominent peaks in the alkenones concentration record occurred during S10 and S6, with no analogs

in the brassicasterol record. On the contrary, brassicasterol displayed maximum concentrations during S16, S7 and S4, at times when the alkenones remained low. This different response of the two marine markers and the timing of sapropels suggests that, during these particular sapropels, specific seawater characteristics and environmental conditions may have favored the contrasting proliferation of coccolithophores and diatoms. It is interesting to note here that the profile of brassicasterol concentration followed quite consistently that of the terrestrial marker C_{26}-ol, whereas alkenones concentrations followed a rather independent evolution (Figure 5).

Phytoplankton community succession has traditionally been explained as a result of the competitive abilities of phytoplankton groups for different nutrients (e.g., silicate, essential for diatom growth but not so for coccolitophores) and their dynamics in the water column (Cermeño et al., 2011; Litchman et al., 2007). Given the observed similarities between C_{26}-ol and brassicasterol fluctuations (Figure 5), it is possible that nutrients supplied through the enhanced terrigenous inputs might have had some influence in stimulating diatom growth. Thus, during sapropels S16, S7 and S4, which are examples of events that involved brassicasterol and C_{26}-ol concentration maxima, the enhanced river runoff during these times may have brought nutrients essential to diatoms, that is, silicon and iron.

Signatures of increased proliferation of diatoms in sapropel sequences have been found particularly in the Eastern Mediterranean Sea, with the presence of diatomaceous remains (e.g., Frydas & Hemleben,, 2007; Kemp et al., 1999), and through high brassicasterol concentrations (e.g., Bouloubassi et al., 1998, 1999). Interestingly, in the latter studies, where C_{37} alkenones were analyzed together with brassicasterol, diatoms were shown to be the dominant phytoplankton contributors during sapropels S5 and S7, whereas coccolithophores dominated during S6. This agrees with our findings in core LC07, where alkenones concentration maximized during S6 (Figure 5). Similarly, a maximum in brassicasterol concentration was also found in LC07 around S7 and also in the vicinity of S5, although in this case it seems to have occurred slightly earlier in time. In a previous study, also on molecular biomarkers associated with sapropels, based in two cores from the Eastern Mediterranean, S6 was also found to be dominated by prymnesiophyte algae and S5 by diatoms (Ten Haven et al., 1987). During S5, high abundances of diatom valves and opal and a decrease in coccoliths were also reported in the Eastern Mediterranean, south of Crete and Turkey (Schrader & Matherne, 1981).

In relation to the most conspicuous C_{37} alkenones concentration maxima in the LC07 record, concurrent with S10 and S6, there are some indications that these sapropels were characterized by remarkable oligotrophic surface water conditions and by less severe bottom water anoxia than other sapropels, as seen through planktonic and benthic foraminiferal fauna (Cita et al., 1977; Melki et al., 2010; Schmiedl et al., 2003). These more oligotrophic surface waters, still within sapropel events, might explain the proliferation of coccolithophore species over diatoms inferred in core LC07, in line with the known ecology of most coccolithophores.

In first instance, the calculation of $\delta^{18}O_{sw\text{-}ivc}$ in our site could provide a semi-quantitative idea of changes in the hydrological cycle over the Central Mediterranean, that may be related to the intensity and position of the westerly winds and the ITCZ. However, when we compare these data with published reconstructions of the position of the westerlies, no clear correspondences are found. For instance, pollen studies at site U1385 in the southwestern Iberian Margin, which lays at a similar latitude than core LC07, suggested a large development of the Iberian Mediterranean forest during the first substages of MIS 7 and during MIS 13 and, hence, a relatively southern position of the westerlies bringing strong winter precipitation to the Mediterranean region (Oliveira et al., 2020; Sánchez-Goñi et al., 2019). In contrast, the low development of the Mediterranean forest identified during MIS 11 (Oliveira et al., 2016) suggests low winter precipitation and, therefore, a relatively northward position of the westerlies in this region. However, at LC07 core, $\delta^{18}O_{sw\text{-}ivc}$ data do not fully match with this picture (Figure 5). If we interpreted them in terms of precipitation/aridity, MIS 12 may indeed look more humid than MIS 11, which contradicts what is known in the area (e.g., Regattieri et al., 2016). This leads us to suggest that salinities in our studied location during these periods may have been controlled by other processes. One possibility is a stronger influence of the less salty surface Atlantic waters in our site, which could be related to the extremely low sea levels at these glacial stages (Figure 5). Indeed, during MIS 12 and MIS 6, the anomalous excursions towards lighter planktonic

foraminifera $\delta^{18}O$, drastically different to the SST record, are the parameters which dominate these same changes in the $\delta^{18}O_{sw\text{-}ivc}$ data (Figure 5).

Altogether, while some of the sapropels may have commonalities in the environmental characteristics and water column properties, it is evident from the literature and from our own results that sapropels are temporally and regionally diverse. The results presented here shed some light on the ecological response of marine phytoplankton to different sapropel conditions. However, more research is needed to better understand the peculiarities of each sapropel event in the different sub-basins of the Mediterranean Sea.

6. Conclusions

We present new molecular biomarker data from the Mediterranean Sea extending back, for the first time, from the present to more than 1 Ma. The reconstruction of SST, terrestrial inputs and changes in phytoplankton composition from the Strait of Sicily represents a unique opportunity to gain knowledge on the climatic evolution of the Mediterranean Sea over these long timescales.

The LC07 SST reconstruction goes back to MIS 28 and shows a total temperature amplitude of ~14°C between the coldest glacials (MIS 10 and 12) and the warmest interglacial (MIS 11). The increase in the 100 kyr-amplitude climate cycles that took place after 430 ka, during the Mid-Brunhes Transition is also depicted in our SST record. From that time, interglacial climates became warmer, as recorded in other basins, but the Central Mediterranean also experienced a pronounced, and less common, decrease in glacial SST minima. Comparison with other alkenone records from nearby sites in the western Mediterranean and Iberian margin shows a strong W-E SST gradient with overall warmer temperatures in the Strait of Sicily. This is indicative of the progressive warming that surface waters experience along their transit from the Strait of Gibraltar to the Central Mediterranean as a result of latitudinal insolation differences between these regions.

Regarding molecular biomarker concentration, the evolution of C_{37} alkenones, brassicasterol and long-chain alcohols was not controlled by glacial/interglacial variability but displayed abrupt maxima, sometimes coeval with the deposition of the Mediterranean sapropels. At these times, an enhanced export production is suggested either by the alkenone or the brassicasterol records but rarely by both biomarkers at the same time. This contrasting evolution of these compounds suggest distinct oceanographic and environmental conditions at each sapropel in the Central Mediterranean that favored the specific proliferation of coccolithophores or diatoms.

Data Availability Statement

Data generated in this work is available at https://data.mendeley.com/datasets/89y57gwbzk/3 archived at the public repository Mendeley as: Martínez-Dios, Ariadna; Pelejero, Carles; Cobacho, Sara; Movilla, Juancho; Dinarès-Turell, Jaume; Calvo, Eva (2021), "Molecular biomarker record of environmental change in the central Mediterranean Sea for the last million years," Mendeley Data, V3, https://doi.org/10.17632/89y57gwbzk.3.

Acknowledgments
Financial support is acknowledged to the Spanish Ministry of Science and Innovation through a Formación de Personal Investigador (FPI) PhD contract to Ariadna Martínez-Dios and research projects SCORE (CGL2015-68194-R) and HICCUP (RTI2018-095083-B-I00). Access to the studied core was kindly provided by the British Ocean Sediment Core Repository (BOSCOR) at the Southampton Oceanography Centre, Southampton, UK. This work acknowledges the "Severo Ochoa Centre of Excellence" accreditation (CEX2019-000928-S). This is a contribution from the Marine Biogeochemistry and Global Change research group (Grant 2017SGR1011, Generalitat de Catalunya). We are grateful to two anonymous reviewers, an associate editor and Ursula Röhl for their detailed and constructive reviews and for the handling of the manuscript.

References

Aïssi, M. (2015). Seamounts and seamount-like structures of Sardinia Channel, Strait of Sicily, Ionian Sea and Adriatic Sea. In M. Rovere, & M. Würtz (Eds.), *Atlas of the Mediterranean seamounts and seamount-like structures* (pp. 187–225): IUCN International Union for Conservation of Nature. https://doi.org/10.2305/IUCN.CH.2015.07.en

Amies, J. D., Rohling, E. J., Grant, K. M., Rodríguez-Sanz, L., & Marino, G. (2019). Quantification of African monsoon runoff during last interglacial sapropel S5. *Paleoceanography and Paleoclimatology*, *34*(8), 1487–1516. https://doi.org/10.1029/2019PA003652

Astraldi, M., Conversano, F., Civitarese, G., Gasparini, G. P., Ribera d'Alcalà, M., & Vetrano, A. (2002). Water mass properties and chemical signatures in the central Mediterranean region. *Journal of Marine Systems*, *33–34*, 155–177. https://doi.org/10.1016/S0924-7963(02)00057-X

Bahr, A., Kaboth, S., Hodell, D., Zeeden, C., Fiebig, J., & Friedrich, O. (2018). Oceanic heat pulses fueling moisture transport towards continental Europe across the mid-Pleistocene transition. *Quaternary Science Reviews*, *179*, 48–58. https://doi.org/10.1016/j.quascirev.2017.11.009

Bahr, A., Kaboth, S., Jiménez-Espejo, F. J., Sierro, F. J., Voelker, A. H. L., Lourens, L., et al. (2015). Persistent monsoonal forcing of Mediterranean Outflow Water dynamics during the late Pleistocene. *Geology*, *43*(11), 951–954. https://doi.org/10.1130/g37013.1

Ballard, R. D., McCann, A. M., Yoerger, D., Whitcomb, L., Mindell, D., Oleson, J., et al. (2000). The discovery of ancient history in the deep sea using advanced deep submergence technology. *Deep Sea Research Part I: Oceanographic Research Papers*, *47*(9), 1591–1620. https://doi.org/10.1016/s0967-0637(99)00117-x

Barth, A. M., Clark, P. U., Bill, N. S., He, F., & Pisias, N. G. (2018). Climate evolution across the Mid-Brunhes Transition. *Climate of the Past*, *14*(12), 2071–2087. https://doi.org/10.5194/cp-14-2071-2018

Batchelor, C. L., Margold, M., Krapp, M., Murton, D. K., Dalton, A. S., Gibbard, P. L., et al. (2019). The configuration of Northern Hemisphere ice sheets through the Quaternary. *Nature Communications*, *10*, 3713. https://doi.org/10.1038/s41467-019-11601-2

Bemis, B. E., Spero, H. J., Bijma, J., & Lea, D. W. (1998). Reevaluation of the oxygen isotopic composition of planktonic foraminifera: Experimental results and revised paleotemperature equations. *Paleoceanography*, *13*, 150–160. https://doi.org/10.1029/98PA00070

Béranger, K., Mortier, L., Gasparini, G.-P., Gervasio, L., Astraldi, M., & Crépon, M. (2004). The dynamics of the Sicily Strait: A comprehensive study from observations and models. *Deep Sea Research Part II: Topical Studies in Oceanography*, *51*(4–5), 411–440. https://doi.org/10.1016/j.dsr2.2003.08.004

Berger, A., Crucifix, M., Hodell, D. A., Mangili, C., McManus, J. F., Otto-Bliesner, B., et al. (2016). Interglacials of the last 800,000 years. *Reviews of Geophysics*, *54*, 162–219. https://doi.org/10.1002/2015RG000482

Bintanja, R., van de Wal, R. S. W., & Oerlemans, J. (2005). Modelled atmospheric temperatures and global sea levels over the past million years. *Nature*, *437*, 125–128. https://doi.org/10.1038/nature03975

Bonanno, A., Placenti, F., Basilone, G., Mifsud, R., Genovese, S., Patti, B., et al. (2014). Variability of water mass properties in the Strait of Sicily in summer period of 1998–2013. *Ocean Science*, *10*, 759–770. https://doi.org/10.5194/os-10-759-2014

Bouloubassi, I., Guehenneux, G., & Rullkötter, J. (1998). Biological marker significance of organic matter origin in sapropels from the Mediterranean Ridge, Site 9691. *Proceedings of the Ocean Drilling Program, Scientific Results*, *160*, 261–269. https://doi.org/10.2973/odp.proc.sr.160.003.1998

Bouloubassi, I., Rullkötter, J., & Meyers, P. A. (1999). Origin and transformation of organic matter in Pliocene–Pleistocene Mediterranean sapropels: Organic geochemical evidence reviewed. *Marine Geology*, *153*, 177–197. https://doi.org/10.1016/S0025-3227(98)00082-6

Brunet, C., Casotti, R., Vantrepotte, V., & Conversano, F. (2007). Vertical variability and diel dynamics of picophytoplankton in the Strait of Sicily, Mediterranean Sea, in summer. *Marine Ecology Progress Series*, *346*, 15–26. https://doi.org/10.3354/meps07017

Budillon, F., Lirer, F., Iorio, M., Macrì, P., Sagnotti, L., Vallefuoco, M., et al. (2009). Integrated stratigraphic reconstruction for the last 80 kyr in a deep sector of the Sardinia Channel (Western Mediterranean). *Deep Sea Research Part II: Topical Studies in Oceanography*, *56*(11–12), 725–737. https://doi.org/10.1016/j.dsr2.2008.07.026

Cacho, I., Grimalt, J. O., & Canals, M. (2002). Response of the Western Mediterranean Sea to rapid climatic variability during the last 50,000 years: A molecular biomarker approach. *Journal of Marine Systems*, *33–34*, 253–272. https://doi.org/10.1016/S0924-7963(02)00061-1

Cacho, I., Grimalt, J. O., Canals, M., Sbaffi, L., Shackleton, N. J., Schönfeld, J., & Zahn, R. (2001). Variability of the western Mediterranean Sea surface temperature during the last 25,000 years and its connection with the Northern Hemisphere climatic changes. *Paleoceanography*, *16*, 40–52. https://doi.org/10.1029/2000PA000502

Cacho, I., Grimalt, J. O., Pelejero, C., Canals, M., Sierro, F. J., Flores, J. A., & Shackleton, N. (1999). Dansgaard-Oeschger and Heinrich event imprints in Alboran Sea paleotemperatures. *Paleoceanography*, *14*(6), 698–705. https://doi.org/10.1029/1999PA900044

Calvo, E., Pelejero, C., & Logan, G. A. (2003). Pressurized liquid extraction of selected molecular biomarkers in deep sea sediments used as proxies in paleoceanography. *Journal of Chromatography, A*, *989*, 197–205. https://doi.org/10.1016/S0021-9673(03)00119-5

Calvo, E., Pelejero, C., Logan, G. A., & De Deckker, P. (2004). Dust-induced changes in phytoplankton composition in the Tasman Sea during the last four glacial cycles. *Paleoceanography*, *19*(2), PA2020. https://doi.org/10.1029/2003PA000992

Calvo, E., Pelejero, C., Pena, L. D., Cacho, I., & Logan, G. A. (2011). Eastern Equatorial Pacific productivity and related-CO_2 changes since the last glacial period. *Proceedings of the National Academy of Sciences*, *108*, 5537–5541. https://doi.org/10.1073/pnas.1009761108

Calvo, E., Villanueva, J., Grimalt, J. O., Boelaert, A., & Labeyrie, L. (2001). New insights into the glacial latitudinal temperature gradients in the North Atlantic. Results from UK37 sea surface temperatures and terrigenous inputs. *Earth and Planetary Science Letters*, *188*(3–4), 11–519. https://doi.org/10.1016/S0012-821X(01)00316-8

Camafort, M., Gràcia, E., & Ranero, C. R. (2020). Quaternary Seismostratigraphy and Tectonosedimentary Evolution of the North Tunisian Continental Margin. *Tectonics*, *39*(11), e2020TC006243. https://doi.org/10.1029/2020TC006243

Cermeño, P., Lee, J., Wyman, K., Schofield, O., & Falkowski, P. (2011). Competitive dynamics in two species of marine phytoplankton under non-equilibrium conditions. *Marine Ecology Progress Series*, *429*, 19–28. https://doi.org/10.3354/meps09088

Ciavatta, S., Kay, S., Brewin, R. J. W., Cox, R., Di Cicco, A., Nencioli, F., et al. (2019). Ecoregions in the Mediterranean Sea through the reanalysis of phytoplankton functional types and carbon fluxes. *Journal of Geophysical Research: Oceans*, *124*, 6737–6759. https://doi.org/10.1029/2019JC015128

Cita, M. B., Vergnaud-Grazzini, C., Robert, C., Chamley, H., Ciaranfi, N., & d'Onofrio, S. (1977). Paleoclimatic record of a long deep sea core from the Eastern Mediterranean. *Quaternary Research*, *8*(2), 205–235. https://doi.org/10.1016/0033-5894(77)90046-1

Conte, M. H., Sicre, M.-A., Rühlemann, C., Weber, J. C., Schulte, S., Schulz-Bull, D., & Blanz, T. (2006). Global temperature calibration of the alkenone unsaturation index (UK′37) in surface waters and comparison with surface sediments. *Geochemistry, Geophysics, Geosystems*, *7*(2), 1–n. https://doi.org/10.1029/2005GC001054

Cortina, A., Grimalt, J. O., Martrat, B., Rigual-Hernández, A., Sierro, F. J., & Flores, J. A. (2016). Anomalous SST warming during MIS 13 in the Gulf of Lions (northwestern Mediterranean Sea). *Organic Geochemistry*, *92*, 16–23. https://doi.org/10.1016/j.orggeochem.2015.12.004

Cortina, A., Sierro, F. J., Flores, J. A., Martrat, B., & Grimalt, J. O. (2015). The response of SST to insolation and ice sheet variability from MIS 3 to MIS 11 in the northwestern Mediterranean Sea (Gulf of Lions). *Geophysical Research Letters*, *42*, 10366–10374. https://doi.org/10.1002/2015GL065539

Danovaro, R., & Boero, F. (2019). Chapter 11-Italian Seas. In C. Sheppard (Ed.), *World seas: An environmental evaluation* (Vol. I, 2nd ed., pp. 283–306). Academic Press. https://doi.org/10.1016/B978-0-12-805068-2.00060-7

de la Vara, A., del Sastre, P. G., Arsouze, T., Gallardo, C., & Gaertner, M. Á. (2019). Role of atmospheric resolution in the long-term seasonal variability of the Tyrrhenian Sea circulation from a set of ocean hindcast simulations (1997–2008). *Ocean Modelling*, *134*, 51–67. https://doi.org/10.1016/j.ocemod.2019.01.004

Di Lorenzo, M., Sinerchia, M., & Colloca, F. (2018). The North sector of the Strait of Sicily: A priority area for conservation in the Mediterranean Sea. *Hydrobiologia*, *821*, 235–253. https://doi.org/10.1007/s10750-017-3389-7

Dinarès-Turell, J., Hoogakker, B. A. A., Roberts, A. P., Rohling, E. J., & Sagnotti, L. (2003). Quaternary climatic control of biogenic magnetite production and eolian dust input in cores from the Mediterranean Sea. *Palaeogeography, Palaeoclimatology, Palaeoecology*, *190*, 195–209. https://doi.org/10.1016/S0031-0182(02)00605-3

Duhamel, M., Colin, C., Revel, M., Siani, G., Dapoigny, A., Douville, E., et al. (2020). Variations in eastern Mediterranean hydrology during the last climatic cycle as inferred from neodymium isotopes in foraminifera. *Quaternary Science Reviews*, *237*, 106306. https://doi.org/10.1016/j.quascirev.2020.106306

Eglinton, T. I., & Eglinton, G. (2008). Molecular proxies for paleoclimatology. *Earth and Planetary Science Letters*, *275*(1–2), 1–16. https://doi.org/10.1016/j.epsl.2008.07.012

Emeis, K.-C., Schulz, H., Struck, U., Rossignol-Strick, M., Erlenkeuser, H., Howell, M. W., et al. (2003). Eastern Mediterranean surface water temperatures and $\delta^{18}O$ composition during deposition of sapropels in the late Quaternary. *Paleoceanography*, *18*, 1005. https://doi.org/10.1029/2000PA000617

Essallami, L., Sicre, M. A., Kallel, N., Labeyrie, L., & Siani, G. (2007). Hydrological changes in the Mediterranean Sea over the last 30,000 years. *Geochemistry, Geophysics, Geosystems*, *8*, 11–n. https://doi.org/10.1029/2007gc001587

Frydas, D., & Hemleben, C. (2007). Opal phytoplankton assemblages of the Late Quaternary sapropel layers S5 and S7 from the southeastern Mediterranean Sea ("Meteor"-Cruise 40/4, Site 67). *Revue de Micropaléontologie*, *50*(2), 169–183. https://doi.org/10.1016/j.revmic.2007.02.002

GEBCO Compilation Group. (2020). *GEBCO 2020 grid*. https://doi.org/10.5285/a29c5465-b138-234d-e053-6c86abc040b9

Giorgi, F. (2006). Climate change hot-spots. *Geophysical Research Letters*, *33*(8), L08707. https://doi.org/10.1029/2006GL025734

Girone, A., Maiorano, P., Marino, M., & Kucera, M. (2013). Calcareous plankton response to orbital and millennial-scale climate changes across the Middle Pleistocene in the western Mediterranean. *Palaeogeography, Palaeoclimatology, Palaeoecology*, *392*, 105–116. https://doi.org/10.1016/j.palaeo.2013.09.005

Grant, K. M., Grimm, R., Mikolajewicz, U., Marino, G., Ziegler, M., & Rohling, E. J. (2016). The timing of Mediterranean sapropel deposition relative to insolation, sea-level and African monsoon changes. *Quaternary Science Reviews*, *140*, 125–141. https://doi.org/10.1016/j.quascirev.2016.03.026

Herbert, T. D. (2003). 6.15—Alkenone paleotemperature determinations. In H. D. Holland, & K. K. Turekian (Eds.), *Treatise on Geochemistry* (1st ed., pp. 391–432). Pergamon. https://doi.org/10.1016/B0-08-043751-6/06115-6

Iacono, R., Napolitano, E., Palma, M., & Sannino, G. (2021). The Tyrrhenian sea circulation: A review of recent work. *Sustainability*, *13*(11), 6371. https://doi.org/10.3390/su13116371

Jouini, M., Béranger, K., Arsouze, T., Beuvier, J., Thiria, S., Crépon, M., & Taupier-Letage, I. (2016). The Sicily Channel surface circulation revisited using a neural clustering analysis of a high-resolution simulation. *Journal of Geophysical Research: Oceans*, *121*(7), 4545–4567. https://doi.org/10.1002/2015JC011472

Kemp, A. E. S., Pearce, R. B., Koizumi, I., Pike, J., & Rance, S. J. (1999). The role of mat-forming diatoms in the formation of Mediterranean sapropels. *Nature*, *398*, 57–61. https://doi.org/10.1038/18001

Konijnendijk, T. Y. M., Ziegler, M., & Lourens, L. J. (2014). Chronological constraints on Pleistocene sapropel depositions from high-resolution geochemical records of ODP Sites 967 and 968. *Newsletters on Stratigraphy*, *47*(3), 263–282. https://doi.org/10.1127/0078-0421/2014/0047

Kornilova, O., & Rosell-Melé, A. (2003). Application of microwave-assisted extraction to the analysis of biomarker climate proxies in marine sediments. *Organic Geochemistry*, *34*, 1517–1523. https://doi.org/10.1016/S0146-6380(03)00155-4

Laskar, J. (1990). The chaotic motion of the solar system: A numerical estimate of the chaotic zones. *Icarus*, *88*(2), 266–291. https://doi.org/10.1016/0019-1035(90)90084-M

Lisiecki, L. E., & Raymo, M. E. (2005). A Pliocene-Pleistocene stack of 57 globally distributed benthic delta O-18 records. *Paleoceanography*, *20*, PA1003. https://doi.org/10.1029/2004PA001071

Litchman, E., Klausmeier, C. A., Schofield, O. M., & Falkowski, P. G. (2007). The role of functional traits and trade-offs in structuring phytoplankton communities: Scaling from cellular to ecosystem level. *Ecology Letters*, *10*(12), 1170–1181. https://doi.org/10.1016/B978-012370518-1/50017-510.1111/j.1461-0248.2007.01117.x

Locarnini, R. A., Mishonov, A. V., Antonov, J. I., Boyer, T. P., Garcia, H. E., Baranova, O. K., et al. (2013). In S. Levitus, & A. Mishonov Technical (Eds.), *World Ocean Atlas 2013, volume 1: Temperature*. *NOAA Atlas NESDIS* (Vol. 73, p. 40). https://doi.org/10.7289/V55X26VD

Marino, M., Girone, A., Maiorano, P., Di Renzo, R., Piscitelli, A., & Flores, J. A. (2018). Calcareous plankton and the mid-Brunhes climate variability in the Alboran Sea (ODP Site 977). *Palaeogeography, Palaeoclimatology, Palaeoecology*, *508*, 91–106. https://doi.org/10.1016/j.palaeo.2018.07.023

Martín-García, G. M., Sierro, F. J., Flores, J. A., & Abrantes, F. (2018). Change in the North Atlantic circulation associated with the mid-Pleistocene transition. *Climate of the Past*, *14*(11), 1639–1651. https://doi.org/10.5194/cp-14-1639-2018

Martrat, B., Grimalt, J. O., Lopez-Martinez, C., Cacho, I., Sierro, F. J., Flores, J. A., et al. (2004). Abrupt temperature changes in the Western Mediterranean over the past 250,000 Years. *Science*, *306*, 1762–1765. https://doi.org/10.1126/science.1101706

Martrat, B., Grimalt, J. O., Shackleton, N. J., de Abreu, L., Hutterli, M. A., & Stocker, T. F. (2007). Four climate cycles of recurring deep and surface water destabilizations on the Iberian margin. *Science*, *317*, 502–507. https://doi.org/10.1126/science.1139994

Mascle, G. H., Tricart, P., Torelli, L., Bouillin, J.-P., Compagnoni, R., Depardon, S., et al. (2004). Structure of the Sardinia Channel: Crustal thinning and tardi-orogenic extension in the Apenninic-Maghrebian orogen; results of the Cyana submersible survey (SARCYA and SARTUCYA) in the western Mediterranean. *Bulletin de la Société Géologique de France*, *175*(6), 607–627. https://doi.org/10.2113/175.6.607

Mauffrey, M.-A., Urgeles, R., Berné, S., & Canning, J. (2017). Development of submarine canyons after the Mid-Pleistocene Transition on the Ebro margin, NW Mediterranean: The role of fluvial connections. *Quaternary Science Reviews*, *158*, 77–93. https://doi.org/10.1016/j.quascirev.2017.01.006

Melki, T., Kallel, N., & Fontugne, M. (2010). The nature of transitions from dry to wet condition during sapropel events in the Eastern Mediterranean Sea. *Palaeogeography, Palaeoclimatology, Palaeoecology*, *291*, 267–285. https://doi.org/10.1016/j.palaeo.2010.02.039

Müller, P. J., & Fischer, G. (2001). A 4-year sediment trap record of alkenones from the filamentous upwelling region off Cape Blanc, NW Africa and a comparison with distributions in underlying sediments. *Deep Sea Research Part I: Oceanographic Research Papers*, *48*(8), 1877–1903. https://doi.org/10.1016/S0967-0637(00)00109-6

Müller, P. J., Kirst, G., Ruhland, G., von Storch, I., & Rosell-Melé, A. (1998). Calibration of the alkenone paleotemperature index based on core-tops from the eastern South Atlantic and the global ocean (60ºN–60ºS). *Geochimica et Cosmochimica Acta*, *62*(10), 1757–1772. https://doi.org/10.1016/S0016-7037(98)00097-0

Muttoni, G., Ravazzi, C., Breda, M., Pini, R., Laj, C., Kissel, C., et al. (2007). Magnetostratigraphic dating of an intensification of glacial activity in the southern Italian Alps during Marine Isotope Stage 22. *Quaternary Research*, *67*(1), 161–173. https://doi.org/10.1016/j.yqres.2006.07.006

Oliveira, D., Desprat, S., Rodrigues, T., Naughton, F., Hodell, D., Trigo, R., et al. (2016). The complexity of millennial-scale variability in southwestern Europe during MIS 11. *Quaternary Research*, *86*(3), 373–387. https://doi.org/10.1016/j.yqres.2016.09.002

Oliveira, D., Desprat, S., Yin, Q., Rodrigues, T., Naughton, F., Trigo, R. M., et al. (2020). Combination of insolation and ice-sheet forcing drive enhanced humidity in northern subtropical regions during MIS 13. *Quaternary Science Reviews*, *247*, 106573. https://doi.org/10.1016/j.quascirev.2020.106573

Onken, R., Robinson, A. R., Lermusiaux, P., Haley, P., & Anderson, L. (2003). Data-driven simulations of synoptic circulation and transports in the Tunisia-Sardinia-Sicily region. *Journal of Geophysical Research*, *108*, 8123. https://doi.org/10.1029/2002JC001348

Osborne, A. H., Marino, G., Vance, D., & Rohling, E. J. (2010). Eastern Mediterranean surface water Nd during Eemian sapropel S5: Monitoring northerly (mid-latitude) versus southerly (sub-tropical) freshwater contributions. *Quaternary Science Reviews*, *29*(19–20), 2473–2483. https://doi.org/10.1016/j.quascirev.2010.05.015

Pasquier, V., Toucanne, S., Sansjofre, P., Dixit, Y., Revillon, S., Mokeddem, Z., & Rabineau, M. (2019). Organic matter isotopes reveal enhanced rainfall activity in Northwestern Mediterranean borderland during warm substages of the last 200 kyr. *Quaternary Science Reviews*, *205*, 182–192. https://doi.org/10.1016/j.quascirev.2018.12.007

Pelejero, C., & Calvo, E. (2003). The upper end of the UK′ 37 temperature calibration revisited. *Geochemistry, Geophysics, Geosystems*, *4*(2), 1014. https://doi.org/10.1029/2002GC000431

Pena, L. D., & Goldstein, S. L. (2014). Thermohaline circulation crisis and impacts during the mid-Pleistocene transition. *Science*, *345*, 318–322. https://doi.org/10.1126/science.1249770

Piva, A., Asioli, A., Andersen, N., Grimalt, J. O., Schneider, R. R., & Trincardi, F. (2008). Climatic cycles as expressed in sediments of the PROMESS1 borehole PRAD1-2, central Adriatic, for the last 370 ka: 2. Paleoenvironmental evolution. *Geochemistry, Geophysics, Geosystems*, *9*(3), Q03R02. https://doi.org/10.1029/2007GC001785

Powley, H. R., Cappellen, P. V., & Krom, M. D. (2017). Nutrient cycling in the Mediterranean Sea: The key to understanding how the unique marine ecosystem functions and responds to anthropogenic pressures. In B. Fuerst-Bjelis (Ed.), *Mediterranean Identities—Environment, Society, Culture*: InTech. https://doi.org/10.5772/intechopen.70878

Puig, P. (2017). Dense shelf water cascading and associated bedforms. In J. Guillén, J. Acosta, F. L. Chiocci, & A. Palanques (Eds.), *Atlas of bedforms in the western mediterranean* (pp. 35–40): Springer International Publishing. https://doi.org/10.1007/978-3-319-33940-5_7

Rampen, S. W., Abbas, B. A., Schouten, S., & Damste, J. S. S. (2010). A comprehensive study of sterols in marine diatoms (Bacillariophyta): Implications for their use as tracers for diatom productivity. *Limnology & Oceanography*, *55*(1), 91–105. https://doi.org/10.4319/lo.2010.55.1.0091

Regattieri, E., Giaccio, B., Galli, P., Nomade, S., Peronace, E., Messina, P., et al. (2016). A multi-proxy record of MIS 11–12 deglaciation and glacial MIS 12 instability from the Sulmona basin (Central Italy). *Quaternary Science Reviews*, *132*, 129–145. https://doi.org/10.1016/j.quascirev.2015.11.015

Rinaldi, E., Buongiorno Nardelli, B., Volpe, G., & Santoleri, R. (2014). Chlorophyll distribution and variability in the Sicily Channel (Mediterranean Sea) as seen by remote sensing data. *Continental Shelf Research*, *77*, 61–68. https://doi.org/10.1016/j.csr.2014.01.010

Rodrigo-Gámiz, M., Martínez-Ruiz, F., Rampen, S. W., Schouten, S., & Sinninghe Damsté, J. S. (2014). Sea surface temperature variations in the western Mediterranean Sea over the last 20kyr: A dual-organic proxy (and LDI) approach. *Paleoceanography*, *29*, 87–98. https://doi.org/10.1002/2013PA002466

Rodrigues, T., Alonso-García, M., Hodell, D. A., Rufino, M., Naughton, F., Grimalt, J. O., et al. (2017). A 1-Ma record of sea surface temperature and extreme cooling events in the North Atlantic: A perspective from the Iberian Margin. *Quaternary Science Reviews*, *172*, 118–130. https://doi.org/10.1016/j.quascirev.2017.07.004

Rogerson, M., Rohling, E. J., Bigg, G. R., & Ramirez, J. (2012). Paleoceanography of the Atlantic-Mediterranean exchange: Overview and first quantitative assessment of climate forcing. *Reviews of Geophysics*, *50*. https://doi.org/10.1029/2011RG000376

Rohling, E. J., Marino, G., & Grant, K. M. (2015). Mediterranean climate and oceanography, and the periodic development of anoxic events (sapropels). *Earth-Science Reviews*, *143*, 62–97. https://doi.org/10.1016/j.earscirev.2015.01.008

Rossignol-Strick, M., & Paterne, M. (1999). A synthetic pollen record of the eastern Mediterranean sapropels of the last 1 Ma: Implications for the time-scale and formation of sapropels. *Marine Geology*, *153*(1–4), 221–237. https://doi.org/10.1016/S0025-3227(98)00080-2

Salgueiro, E., Voelker, A. H. L., de Abreu, L., Abrantes, F., Meggers, H., & Wefer, G. (2010). Temperature and productivity changes off the western Iberian margin during the last 150 ky. *Quaternary Science Reviews*, *29*(5–6), 680–695. https://doi.org/10.1016/j.quascirev.2009.11.013

Sammari, C., Millot, C., Taupier-Letage, I., Stefani, A., & Brahim, M. (1999). Hydrological characteristics in the Tunisia–Sardinia–Sicily area during spring 1995. *Deep-Sea Research Part A Oceanographic Research Papers*, *46*, 1671–1703. https://doi.org/10.1016/S0967-0637(99)00026-6

Sánchez-Goñi, M. F., Ferretti, P., Polanco-Martínez, J. M., Rodrigues, T., Alonso-García, M., Rodríguez-Tovar, F. J., et al. (2019). Pronounced northward shift of the westerlies during MIS 17 leading to the strong 100-kyr ice age cycles. *Earth and Planetary Science Letters*, *511*, 117–129. https://doi.org/10.1016/j.epsl.2019.01.032

Schmiedl, G., Mitschele, A., Beck, S., Emeis, K.-C., Hemleben, C., Schulz, H., et al. (2003). Benthic foraminiferal record of ecosystem variability in the eastern Mediterranean Sea during times of sapropel S5 and S6 deposition. *Palaeogeography, Palaeoclimatology, Palaeoecology*, *190*, 139–164. https://doi.org/10.1016/S0031-0182(02)00603-X

Schrader, H., & Matherne, A. (1981). Sapropel formation in the Eastern Mediterranean Sea: Evidence from Preserved Opal Assemblages. *Micropaleontology*, *27*(2), 191–203. https://doi.org/10.2307/1485285

Sicre, M. A., Siani, G., Genty, D., Kallel, N., & Essallami, L. (2013). Seemingly divergent sea surface temperature proxy records in the central Mediterranean during the last deglaciation. *Climate of the Past*, *9*(3), 1375–1383. https://doi.org/10.5194/cp-9-1375-2013

Sierro, F. J., Hodell, D. A., Andersen, N., Azibeiro, L. A., Jimenez-Espejo, F. J., Bahr, A., et al. (2020). Mediterranean overflow over the last 250 kyr: Freshwater forcing from the tropics to the ice sheets. *Paleoceanography and Paleoclimatology*, *35*(9), e2020PA003931. https://doi.org/10.1029/2020PA003931

Sierro, F. J., Hodell, D. A., Curtis, J. H., Flores, J. A., Reguera, I., Colmenero-Hidalgo, E., et al. (2005). Impact of iceberg melting on Mediterranean thermohaline circulation during Heinrich events. *Paleoceanography*, *20*, PA2019. https://doi.org/10.1029/2004PA001051

Sprovieri, M., Di Stefano, E., Incarbona, A., Manta, D. S., Pelosi, N., d'Alcalà, M. R., & Sprovieri, R. (2012). Centennial-to millennial-scale climate oscillations in the Central-Eastern Mediterranean Sea between 20,000 and 70,000 years ago: Evidence from a high-resolution geochemical and micropaleontological record. *Quaternary Science Reviews*, *46*, 126–135. https://doi.org/10.1016/j.quascirev.2012.05.005

Taylforth, J. E., McCay, G. A., Ellam, R., Raffi, I., Kroon, D., & Robertson, A. H. F. (2014). Middle Miocene (Langhian) sapropel formation in the easternmost Mediterranean deep-water basin: Evidence from northern Cyprus. *Marine and Petroleum Geology*, *57*, 521–536. https://doi.org/10.1016/j.marpetgeo.2014.04.015

Ten Haven, H. L., Baas, M., De Leeuw, J. W., & Schenck, P. A. (1987). Late Quaternary Mediterranean sapropels, I—On the origin of organic matter in sapropel S7. *Marine Geology*, *75*(1–4), 137–156. https://doi.org/10.1016/0025-3227(87)90100-9

Ternois, Y., Sicre, M.-A., Boireau, A., Marty, J.-C., & Miquel, J.-C. (1996). Production pattern of alkenones in the Mediterranean Sea. *Geophysical Research Letters*, *23*(22), 3171–3174. https://doi.org/10.1029/96GL02910

Toucanne, S., Angue Minto'o, C. M., Fontanier, C., Bassetti, M.-A., Jorry, S. J., & Jouet, G. (2015). Tracking rainfall in the northern Mediterranean borderlands during sapropel deposition. *Quaternary Science Reviews*, *129*, 178–195. https://doi.org/10.1016/j.quascirev.2015.10.016

Tzedakis, P. C., Hooghiemstra, H., & Pälike, H. (2006). The last 1.35 million years at Tenaghi Philippon: Revised chronostratigraphy and long-term vegetation trends. *Quaternary Science Reviews*, *25*(23–24), 3416–3430. https://doi.org/10.1016/j.quascirev.2006.09.002

Vázquez-Riveiros, N., Waelbroeck, C., Skinner, L., Duplessy, J. C., McManus, J. F., Kandiano, E. S., & Bauch, H. A. (2013). The "MIS 11 paradox" and ocean circulation: Role of millennial scale events. *Earth and Planetary Science Letters*, *371–372*, 258–268. https://doi.org/10.1016/j.epsl.2013.03.036

Villanueva, J., Pelejero, C., & Grimalt, J. O. (1997). Clean-up procedures for the unbiased estimation of C37 alkenone sea surface temperatures and terrigenous n-alkane inputs in paleoceanography. *Journal of Chromatography, A*, *757*(1–2), 145–151. https://doi.org/10.1016/S0021-9673(96)00669-3

Volkman, J. K., Barrett, S. M., Blackburn, S. I., Mansour, M. P., Sikes, E. L., & Gelin, F. (1998). Microalgal biomarkers; a review of recent research developments. *Organic Geochemistry*, *29*(5–7), 1163–1179. https://doi.org/10.1016/S0146-6380(98)00062-X

Wu, J., Böning, P., Pahnke, K., Tachikawa, K., & de Lange, G. J. (2016). Unraveling North-African riverine and eolian contributions to central Mediterranean sediments during Holocene sapropel S1 formation. *Quaternary Science Reviews*, *152*, 31–48. https://doi.org/10.1016/j.quascirev.2016.09.029

Wu, J., Filippidi, A., Davies, G. R., & de Lange, G. J. (2018). Riverine supply to the eastern Mediterranean during last interglacial sapropel S5 formation: A basin-wide perspective. *Chemical Geology*, *485*, 74–89. https://doi.org/10.1016/j.chemgeo.2018.03.037

Zhao, Y., Colin, C., Liu, Z., Bonneau, L., & Siani, G. (2016). Climate forcing of terrigenous sediment input to the central Mediterranean Sea since the early Pleistocene. *Palaeogeography, Palaeoclimatology, Palaeoecology*, *442*, 23–35. https://doi.org/10.1016/j.palaeo.2015.11.006

Ziegler, M., Tuenter, E., & Lourens, L. J. (2010). The precession phase of the boreal summer monsoon as viewed from the eastern Mediterranean (ODP Site 968). *Quaternary Science Reviews*, *29*(11–12), 1481–1490. https://doi.org/10.1016/j.quascirev.2010.03.011

Zwiep, K. L., Hennekam, R., Donders, T. H., van Helmond, N. A. G. M., de Lange, G. J., & Sangiorgi, F. (2018). Marine productivity, water column processes and seafloor anoxia in relation to Nile discharge during sapropels S1 and S3. *Quaternary Science Reviews*, *200*, 178–190. https://doi.org/10.1016/j.quascirev.2018.08.026